

Tetrahedron Report Number 547

# New Mechanistic and Synthetic Aspects of Singlet Oxygen Chemistry

Edward L. Clennan\*

Department of Chemistry, University of Wyoming, Laramie, WY 82071, USA

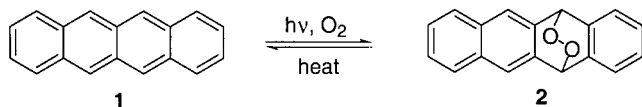
Received 17 July 2000

## Contents

1. Introduction	9151
2. The Singlet Oxygen Ene Reaction	9152
3. Substituent Effects	9155
3.1. Steric effects	9155
3.2. Electronic effects	9159
3.3. Hydrogen bonding effects	9163
4. Environmental Effects	9166
4.1. Solvent effects	9166
4.2. Zeolites	9167
4.3. Micelles, vesicles, and microheterogeneous biological structures	9172
4.4. Nafion membranes	9173
4.5. Miscellaneous efforts to improve regio- and/or stereoselectivity	9174
5. Conclusion and Practical Considerations	9176

## 1. Introduction

It appears that the earliest description of a singlet oxygen reaction was made by Fritzsche in 1867.<sup>1</sup> He reported that naphthalene, **1**, reacted in the presence of light and oxygen to give a material which could regenerate **1** when heated. In 1867 the identity of the reactive oxygen species and the structure of the naphthalene adduct were both unknown. Evidence for a metastable, reactive state of the oxygen molecule was not generated until the 1930's with the report of the elegant and now classic experiments of Kautsky and coworkers,<sup>2–4</sup> and the Fritzsche naphthalene adduct was not conclusively identified as endoperoxide **2** (Scheme 1) until 1976.<sup>5</sup>

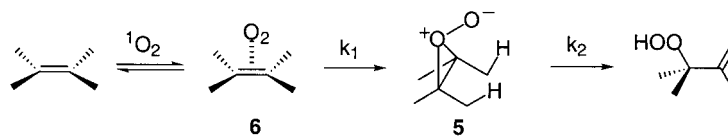


Scheme 1.

\* Tel.: +307-766-6667; fax: +307-766-2807;  
e-mail: clennane@uwyo.edu

Singlet oxygen research blossomed in the 1960's and 1970's and many of the basic mechanistic details of its archetypical 2+2, 4+2, ene, and sulfide oxidation reactions as well as its photophysical behavior had been established by the mid-1980's. Three monographs<sup>5,6</sup> were published during this time period culminating in a detailed 4 volume monograph entitled 'Singlet  $O_2$ '<sup>7</sup> which provide a useful summary of the rapid developments in this important field.

Recent research efforts, stimulated by the recognition that the allylic hydroperoxide and endoperoxide products of the ene and 4+2 reactions are important building blocks for synthetic organic chemistry, have turned to studies designed to enhance the regio- and stereoselectivity of these important reactions.<sup>7–12</sup> These studies, for the most part, have focused on the utilization of substituents and environmental effects to influence the direction of approach of singlet oxygen to the stereogenic faces of the substrate molecules. The success of the substituent effect approach is a result of the sensitivity of singlet oxygen to a variety of factors including: (1) steric effects, (2) electronic effects, and (3) hydrogen bonding effects.<sup>13</sup> On the other hand, the success of the environmental approach is primarily due to the ability of supramolecular systems to organize and to provide



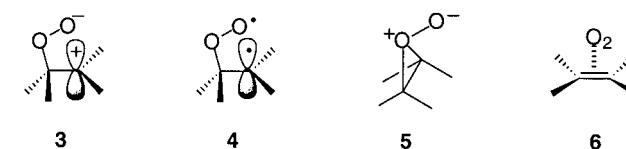
Scheme 2.

limited access to the substrate molecules and, in part, to the ability of the environment to selectively stabilize intermediates on the reaction surface.

Our approach in this report is to examine the ability of substituents to direct the regio- and stereochemistry of the singlet oxygen ene, and to a smaller extent, of the 4+2 cycloaddition reaction. We will also critically examine the efficiencies of supramolecular systems including micelles, cyclodextrins, and zeolites to accomplish these same goals. It is our hope that the description of these substituent and environmental effects will stimulate further work to improve on the already impressive regio- and stereoselectivity of singlet oxygen reactions. First, however, we will briefly review the important mechanistic features of the singlet oxygen ene reaction that will provide the foundation to understand the substituent and environmental effects.

## 2. The Singlet Oxygen Ene Reaction

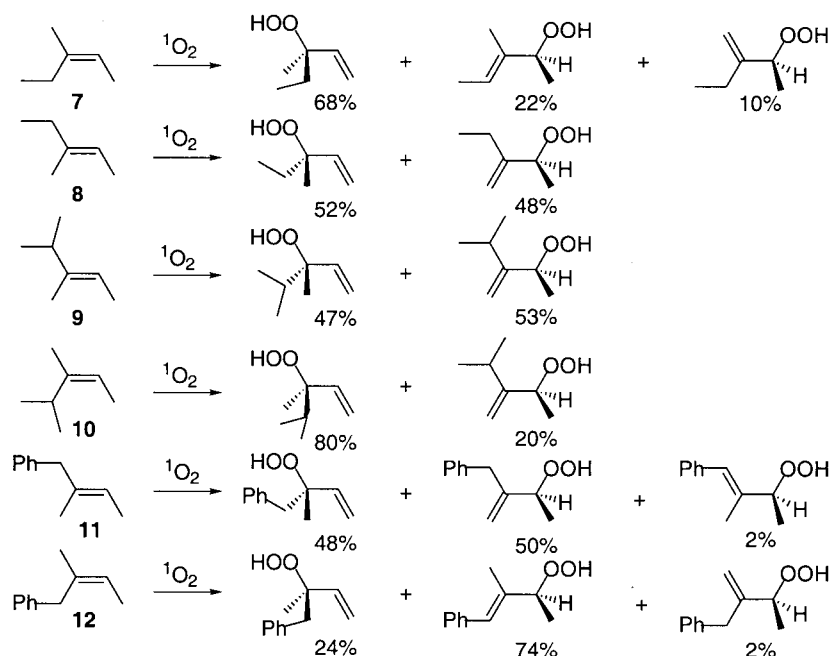
Since the initial report of the singlet oxygen ene reaction in the 1940's<sup>14</sup> both concerted and stepwise mechanisms have been suggested.<sup>15</sup> The stepwise pathways have invoked zwitterionic, **3**, biradical, **4**, peroxide, **5**, and exciplex, **6**, intermediates. Theoretical studies have been unable to distinguish between these mechanistic possibilities but experimental work clearly favors a stepwise pathway.



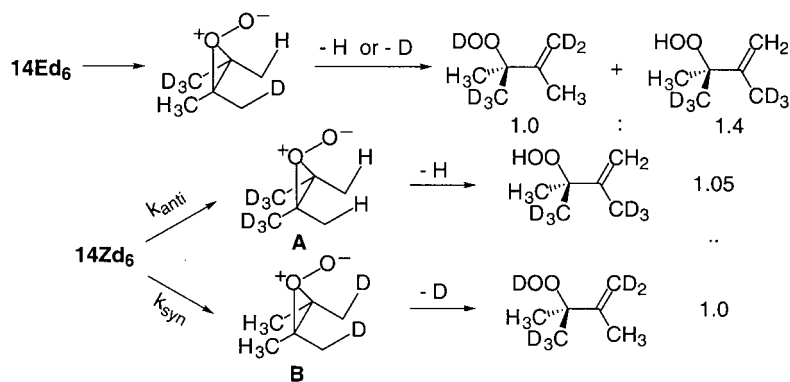
A stepwise mechanism that is supported by a considerable amount of experimental results is shown in Scheme 2. It is our contention that this mechanism provides a suitable template for the design of new regio- and stereospecific singlet oxygen ene reaction systems.

Experimental data that support this mechanism includes the following:

*Evidence in support of an exciplex intermediate, 6.* In 1985 Hurst, Wilson, and Schuster<sup>16</sup> pointed out that even reasonably electron rich olefins react with singlet oxygen at rates  $10^3$  less than diffusion control and as a consequence many non-productive encounters between singlet oxygen and the olefin must occur. They went on to speculate that these encounters could involve an exciplex intermediate. Gorman and coworkers also pointed out that small or even slightly negative activation enthalpies and highly negative activation entropies, which are characteristic of singlet oxygen reactions, are also characteristics of reactions involving rapid and reversibly formed exciplexes.<sup>17</sup> These workers also provided compelling experimental evidence for



Scheme 3.



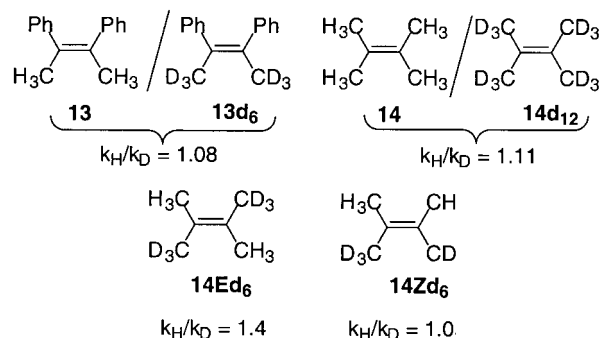
Scheme 4.

exciplex formation. In particular they were able to kinetically detect temperature regions where the exciplex reacts as rapidly as it forms (diffusion limit) and where the dissociation of the exciplex is much faster than its reaction (preequilibrium limit). Remarkably however, these authors refused to concede that any other intermediate, other than the reversibly formed exciplex (demonstrated in the case of tetramethylethylene),<sup>17</sup> was required on the reaction surface despite the compelling evidence for an irreversibly formed perezoxide presented below.

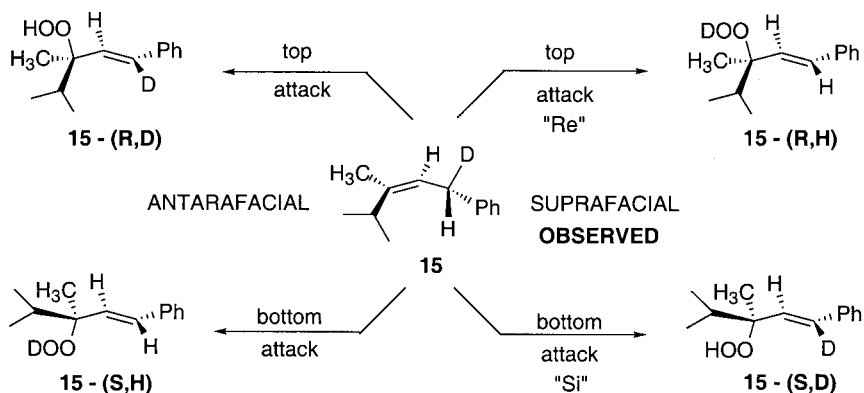
*Evidence against an open zwitterion intermediate 3 or diradical intermediate 4.* Markovnikov directing effects do not play a major role in determining the regiochemistry of the reaction; i.e. the highly electrophilic singlet oxygen does not have an overriding propensity to add to the least substituted end of trisubstituted olefins to generate the more stable tertiary carbocation or radical intermediate. Regioselectivity for addition to the less substituted end of the double bond in the trisubstituted olefins **7–12** (Scheme 3) changes from over 75% in **12** to only 20% in **10**.<sup>15</sup> Consequently, there is no evidence of substantial charge buildup in the transition state for hydrogen abstraction.

*Evidence in support of a perezoxide intermediate, 5.* A compelling body of evidence supports the presence of a perezoxide on the singlet oxygen ene reaction surface. Perhaps the most compelling is the Stephenson inter-/intra-molecular isotope effect test,<sup>18,19</sup> which requires an irreversibly formed intermediate with the symmetry of a perezoxide. In particular, the intermolecular isotope effects

$k_H/k_D$  for **13/13d<sub>6</sub>**<sup>20</sup> and **14/14d<sub>12</sub>** are smaller than the intramolecular isotope effect for **14Ed<sub>6</sub>**.<sup>21</sup> (Scheme 4) This requires that there be distinct rate and product determining steps. A concerted reaction, on the other hand, should show identical inter- and intramolecular isotope effects since the rate and product determining steps are one and the same.



Furthermore, a comparison of intramolecular isotope effects in **14Ed<sub>6</sub>** and **14Zd<sub>6</sub>** (Scheme 4) demonstrates that the product isotope effect exhibits a stereochemical dependence; an isotope effect is only observed when the competing isotopes are *cis* to one another, as in **14Ed<sub>6</sub>**.<sup>22</sup> This is exactly the result one would anticipate if a perezoxide is a bonafide intermediate. Addition of singlet oxygen to **14Ed<sub>6</sub>** gives only one perezoxide intermediate that still has a choice to abstract hydrogen or deuterium in the rate-determining step, and as a consequence a substantial isotope effect is observed (Scheme 4). On the other hand **14Zd<sub>6</sub>**,



Scheme 5.

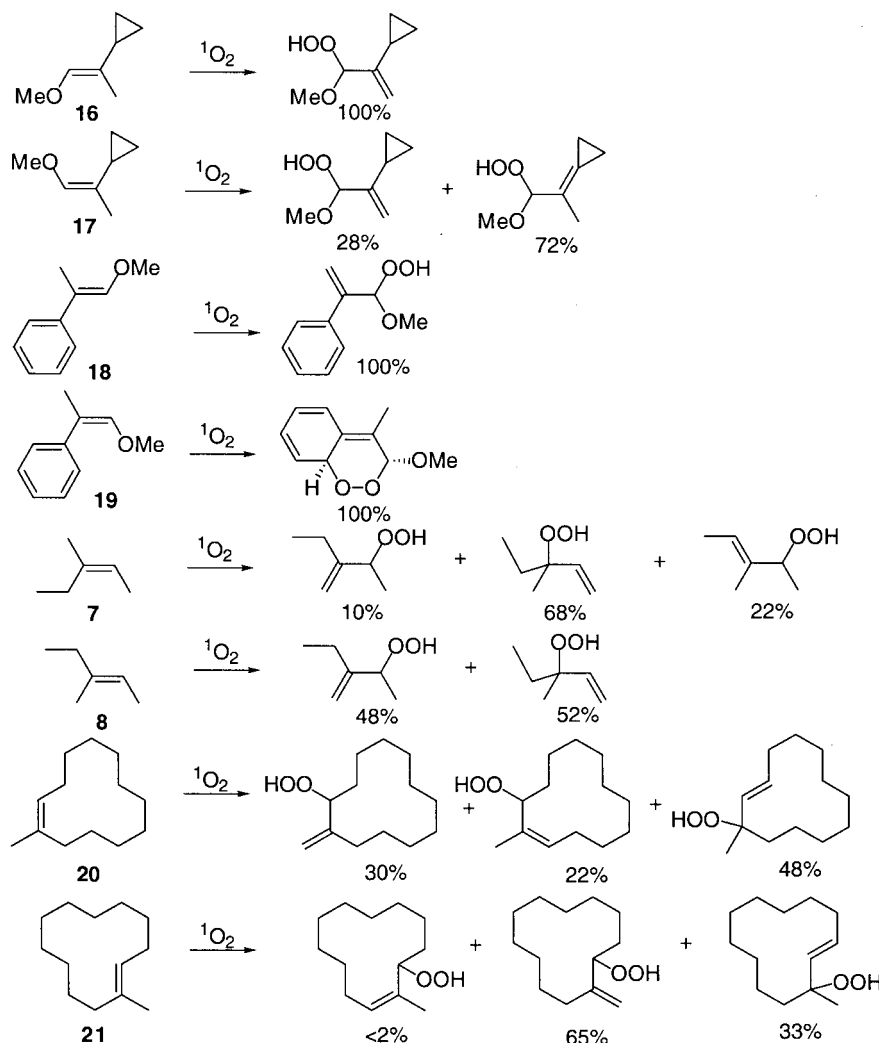
forms two distinct perepoxides (**A** and **B** in Scheme 4) neither of which have a choice to discriminate between isotopes in the product-determining step. Since neither  $k_{syn}$  nor  $k_{anti}$  involve breakage of a carbon–isotope bond  $k_{syn}/k_{anti}$  should be approximately 1 (i.e.  $A/B \approx 1$ ) and no isotope effect should be observed, consistent with the experimental results. This analysis requires that perepoxides **A** and **B** (Scheme 4) do not interconvert either by inversion or by reversion to the exciplex **6** (i.e. the microscopic reaction step represented by  $k_1$  in Scheme 2 is essentially irreversible).

The singlet oxygen ene reaction is a suprafacial process characterized by the addition of oxygen and abstraction of hydrogen from the same face of the olefinic  $\pi$ -system. (Scheme 5) This stereochemical feature was elegantly demonstrated using chiral olefin **15**, which is available in known optical purity.<sup>23</sup> Photooxidation of **15** resulted in 82% abstraction from the benzylic group and exclusive formation of the *trans* rather than the *cis* allylic hydroperoxide. The depicted enantiomer of **15** (Scheme 5) reacted suprafacially with singlet oxygen from the Re (top attack) face to give deuterium abstraction and from the Si (bottom attack) face to give hydrogen abstraction. No products from

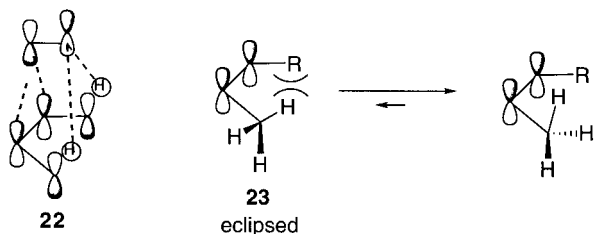
antarafacial attack were observed. A suprafacial process is that expected for the perepoxide, **5**, which is geometrically precluded from abstraction of a hydrogen anti (antiperiplanar or anticlinal) to the C–O bond in the perepoxide ring.

Singlet oxygen has a propensity to abstract hydrogen from the most congested side of an olefin. This phenomenon, which has subsequently become known as the ‘*cis* effect’ was first recognized in enol ethers by Conia<sup>24</sup> and Foote.<sup>25</sup> The methoxy group in enol ethers **16**–**19** induces predominant reaction at the *cis* olefinic substituent even when this involves inherently unfavorable formation of a double bond exocyclic to a cyclopropane ring (e.g. **17**) or loss of aromaticity (i.e. the methoxy group in **19** promotes 4+2 cycloaddition to the *cis* phenyl group in preference to hydrogen abstraction from the *trans* methyl group). This ‘*cis* effect’ was also observed in acyclic<sup>26</sup> and cyclic<sup>27</sup> aliphatic olefins as depicted by **7**, **8**, **20** and **21** (Scheme 6).

Two different models have been suggested to explain the ‘*cis* effect’ one of which provides direct support for a perepoxide intermediate. In the Stephenson/Fukui model<sup>28,29</sup> a favorable HOMO–LUMO interaction between the trailing oxygen in the incipient perepoxide and the allylic hydrogens



Scheme 6.



Scheme 7.

**Table 1.** Kinetic data for the reactions of singlet oxygen with aliphatic olefins (in CS<sub>2</sub>).<sup>16)</sup>

Olefin	$\Delta H^\ddagger$ (kcal/mol)	$\Delta S^\ddagger$ (eu) <sup>a</sup>	$k_r$ (M <sup>-1</sup> s <sup>-1</sup> )
	1.6	-35	4.8×10 <sup>4</sup>
	0.3	-45	7.2×10 <sup>3</sup>
	2.0	-34	3.9×10 <sup>4</sup>
	0.4	-42	7.7×10 <sup>3</sup>
			4.1×10 <sup>4</sup> <sup>b</sup>
			2.1×10 <sup>4</sup> <sup>b</sup>

<sup>a</sup> Normalized for number of reactive sites.<sup>b</sup> From reference<sup>34</sup>.

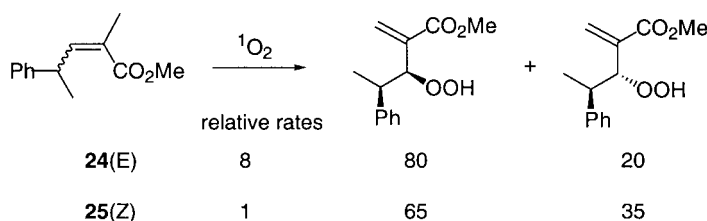
association of the pendant oxygen in the perepoxide with the *cis* hydrogens (the ‘*cis* effect’) as shown by the data in Table 1. The reactions of *cis*-olefins are characterized by less negative activation entropies and reaction rates that are approximately 2–8 times larger than their *trans* isomers. Adam and Nestler<sup>32</sup> recently pointed out that this phenomenon is also observed in trisubstituted olefins as exemplified by the 8 fold slower reaction of the *Z* acrylic ester, **25**, in comparison to its *E* isomer, **24** (Scheme 8). The more negative entropies of activation for the *trans* olefins imply that the transition states in these reactions are more organized,<sup>33</sup> or possibly further along the reaction coordinate, than for the *cis* olefins.<sup>13</sup>

### 3. Substituent Effects

It is the relative free energies of the competing transition states that determine the regio- and stereochemistry of singlet oxygen reactions. Substituent effects play a major role, but not the only role, in determining the free energy differences between two transition states. The origin of these substituent effects is often very complex and several factors may be operating simultaneously. Nevertheless, in the following discussion we have artificially dissected substituent effects into steric, electronic, and hydrogen bonding effects.

#### 3.1. Steric effects

It has been known for many years that steric effects play a



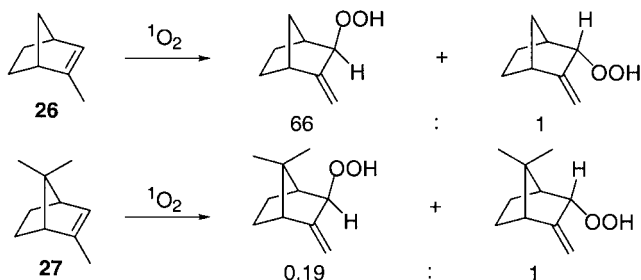
Scheme 8.

is maximized on the more congested side of the olefin. This is depicted pictorially by **22** in Scheme 7, which shows the frontier orbital interactions between the  $\pi^*$ -like singlet oxygen LUMO and the olefin HOMO. In an interesting suggestion, Houk and coworkers<sup>30</sup> suggested that the barrier to rotate the allylic hydrogen to the perpendicular geometry favorable for abstraction plays a dominant role in dictating the regiochemistry of the reactions. This phenomenon could be operating in the perepoxide but could also play a part in a concerted reaction as well. Their calculations demonstrated that the eclipsed geometry of a methyl group (**23** in Scheme 7) is destabilized and its rotation barrier lowered when buttressed by a *cis* substituent. The Houk model has been criticized and its inability to predict the correct regiochemistry when sterically demanding groups are present has been noted.<sup>31</sup> However, regardless of the origin of the ‘*cis* effect’, it provides a useful tool to engineer the regiochemistry of the singlet oxygen ene reaction.

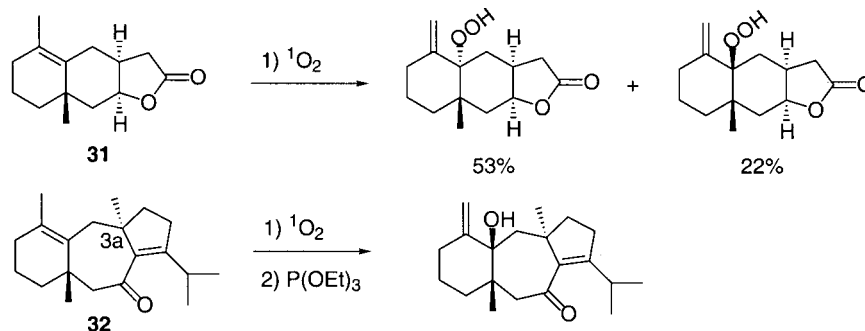
There are kinetic implications that accompany the

large role in singlet oxygen reactions. For example, in the early 1970’s Jefford and coworkers reported that the *exo/endo* hydroperoxide ratio formed in the photooxidation of 2-methylnorborn-2-ene, **26**, is reversed in its 7,7-dimethyl derivative **27**.<sup>35,36</sup> (Scheme 9)

Steric effects can operate at various locations on the reaction



Scheme 9.

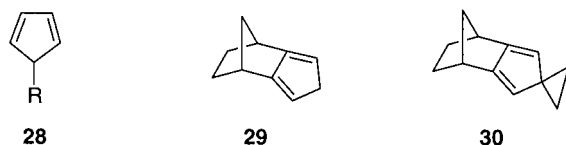


Scheme 10.

surface for the mechanism depicted in Scheme 2. In particular steric effects can operate in: (i) the exciplex or in the transition state for its formation, (ii) in the perepoxide or in the transition state for its formation, or (iii) in the transition state for hydrogen abstraction. We will briefly discuss steric interactions at each of these stationary points on the reaction surface and then examine a case study where steric effects were cleverly designed to enhance regio- and stereochemistry of several singlet oxygen reactions.

*Steric effects in the exciplex.* In reactions in which exciplex formation is reversible singlet oxygen can sample the various diastereomeric exciplexes and choose the sterically least destabilized. In reactions in which exciplex formation is irreversible diastereoselectivity is dictated by steric approach control. Gorman and Adam and coworkers<sup>8,17</sup> have pointed out that ‘slow quenchers’ such as olefins (e.g. 2,3-dimethyl-2-butene) react via reversibly formed exciplexes while ‘rapid quenchers’ such as cyclopentadienes or  $\beta$ -carotene react via rate determining formations of exciplexes.

In the case of rapid quenchers such as cyclopentadiene, **28**, isodicyclopentadiene, **29**, and its spirocyclopropyl derivative, **30**, the magnitude of the steric approach control is a function of the position of the transition state on the reaction surface. For example, isodicyclopentadiene, **29**, and its spirocyclopropyl derivative, **30**, react with singlet oxygen nearly an order of magnitude faster than cyclopentadiene [( $k=2.3\times 10^7$ ,  $1.5\times 10^8$ , and  $1.3\times 10^8$   $M^{-1} s^{-1}$ , respectively, for **28** (R=H), **29**, and **30**) as a result of strain induced enhanced reactivity.<sup>37,38</sup> As a consequence, substituted cyclopentadienes, **28**, exhibit dramatic steric effects while little or no facial selectivity is observed during the reactions of **29** or **30** with singlet oxygen.



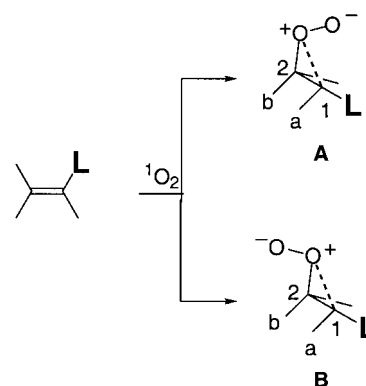
Slow quenchers such as olefins, however, are more reliable in their exhibition of steric effects. Olefins **31** and **32**, for example, which are undoubtedly slow quenchers of singlet oxygen, exhibit dramatic steric effects. The angular methyl group in **31** destabilizes the  $\beta$ -exciplex relative to the  $\alpha$ -exciplex and as a consequence the  $\alpha$ -allylic hydro-

peroxide product dominates.<sup>39</sup> On the other hand the 7-membered ring in **32** (Scheme 10) twists the angular methyl group out away from the  $\beta$ -face while at the same time pushing the methyl group at 3a into the  $\alpha$  face of the olefin. The net result is stabilization of the  $\beta$ -exciplex relative to the  $\alpha$ -exciplex and exclusive formation of the  $\beta$ -allylic hydroperoxide.

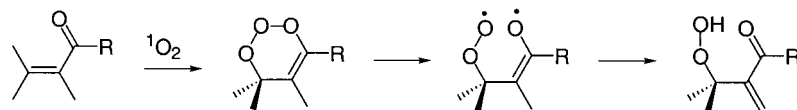
*Steric effects in the perepoxide.* Suitably substituted olefins can react with singlet oxygen to give two diastereomeric perepoxides as illustrated in Scheme 11. A sterically demanding substituent L (large) interacts with the perepoxide ring system in two different ways; (1) a destabilizing interaction between L and the pendant oxygen ( $O^-$ ) destabilizes perepoxide diastereomer **A** relative to perepoxide diastereomer **B**, and (2) an interaction between the perepoxide ring system and L lengthens the  $O^+-C_1$  bond length. As a consequence of this interaction the  $O^+-C_1$  is weakened relative to the  $O^+-C_2$  bond and has a greater propensity to open to give preferential hydrogen abstraction from the end of the double bond bearing the substituent L. This phenomenon has been called the ‘geminal effect’ since the L group directs hydrogen abstraction to the group geminal to it on the double bond.<sup>40</sup>

The L group can be a carbonyl (carboxylic acid,<sup>41</sup> aldehyde,<sup>42</sup> ketone,<sup>43–45</sup> amide,<sup>46</sup> or ester<sup>47</sup>), an alkyl group,<sup>48–52</sup> an aryl group,<sup>53</sup> a sulfinyl group,<sup>54</sup> a silyl group,<sup>55–58</sup> a stannyl group,<sup>59,60</sup> a cyano group,<sup>46</sup> or an iminyl group.<sup>61,62</sup>

The mechanism in Scheme 11 replaces an older mechanism which was proposed in order to rationalize the dramatic

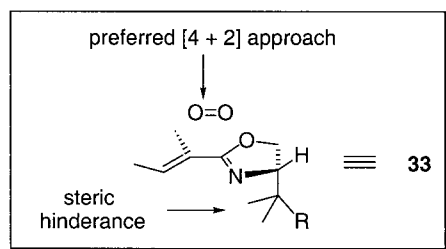


Scheme 11.



Scheme 12.

geminal selectivity observed in the ene reactions of a series of  $\alpha,\beta$ -unsaturated ketones and lactones.<sup>43</sup> In this older mechanism a 4+2 cycloaddition to the enone functional group, to form a trioxene, followed by homolytic cleavage of an O–O bond forces geminal hydrogen abstraction. (Scheme 12) This mechanism was supported by the fact that enones structurally confined to a *s-trans* conformation were unreactive ene substrates. Adam and coworkers pointed out however that this 4+2 cycloaddition mechanism would predict a diastereoselective ene reaction of oxazolidine substituted olefin **33** contrary to the experimental observation.<sup>63</sup> Foote and coworkers<sup>44</sup> also reported that *s-trans* fixed enones react with singlet oxygen with rate constants comparable in magnitude to *s-cis* substrates. (e.g. 2,3-dimethyl-2,3-cyclopentenone [ $k_T=7.8 \times 10^4 \text{ M}^{-1} \text{ s}^{-1}$ ; *s-trans*], and R(+)-pulegone [ $k_T=8 \times 10^5 \text{ M}^{-1} \text{ s}^{-1}$ ; *s-cis*]) Consequently, the simple steric rationale in Scheme 11 along with the ‘*cis* effect’ (vide supra) would appear to provide a satisfying rationale for the regioselectivity, including the ‘geminal effect’, observed during photooxidations of acyclic and some cyclic olefins.<sup>52</sup>



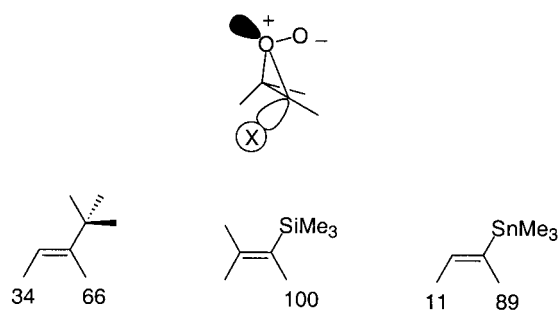
The ability of the small axially symmetric cyano substituent to direct hydrogen abstraction exclusively to the geminal position, however, suggests that the rationale depicted in Scheme 11 is still not complete and that another factor must also be operating.<sup>46</sup> A possible candidate for this other factor is a stereoelectronic model first proposed to rationalize the geminal selectivity in the ene reactions of vinylsilanes.<sup>56</sup> This model suggests that the HOMO of the perepoxide is a linear combination of the lone pair orbital on oxygen and a  $\sigma$ -orbital localized for the most part on the bond to the substituent (Scheme 13). This HOMO is antibonding and any substituent that reduces the energy difference between the oxygen lone pair orbital and the C-substituent bond would increase the antibonding interaction and favor cleavage of the adjacent C–O bond. Alternatively, and perhaps more likely, the resonance stabilization of the  $\alpha,\beta$ -unsaturated nitrile product could be determining the regiochemistry of the hydrogen abstraction.

The steric effect (Scheme 11) and the stereoelectronic effect (Scheme 13) are working in opposite directions for the *t*Bu-, Me<sub>3</sub>Si-, and Me<sub>3</sub>Sn- substituents.<sup>59</sup> If the stereoelectronic effect were acting alone geminal selectivity should be the

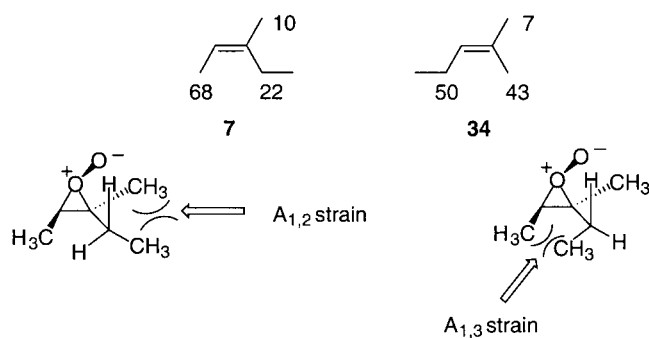
highest for the Me<sub>3</sub>Sn- substituent since the C–Sn bond has the highest energy  $\sigma$ -orbital. If the steric effect were operating alone geminal selectivity should increase in the order Me<sub>3</sub>Sn- < Me<sub>3</sub>Si- < *t*Bu- since the longer Sn–C and Si–C bonds decrease the effective size of these substituents. The net result of these two opposing effects is a maximum in regioselectivity for the vinylsilane (Scheme 13).

*Steric effects in the hydrogen abstraction step.* Two important criteria must be met for facile formation of the allylic hydroperoxide in the hydrogen abstraction step: (1) the allylic hydrogen must be accessible to the pendant oxygen, and (2) as the allylic hydrogen is removed, energetically favorable overlap must be maintained between the breaking C–H bond and the incipient p-orbital forming as a result of C–O cleavage in the perepoxide. Consequently, the allylic hydrogen must either be perpendicular to the  $\pi$ -system in the substrate or the allylic carbon must be able to rotate to place it in a geometrical favorable position in the perepoxide. Steric effects can impede attainment of this favorable geometry. For example, the amount of hydrogen abstraction from the ethyl group in **7** is significantly less than from the ethyl group in its isomer **34** because of the developing destabilizing steric interactions ( $A_{1,2}$  strain)<sup>64</sup> between the two methyl groups in the developing allylic hydroperoxide<sup>58</sup> (Scheme 14). Allylic strain ( $A_{1,3}$  strain)<sup>64</sup> can also play an important role in determining the stereochemistry of the incipient double bond and the choice of which hydrogen is abstracted in the perepoxide<sup>12</sup> (Scheme 14).

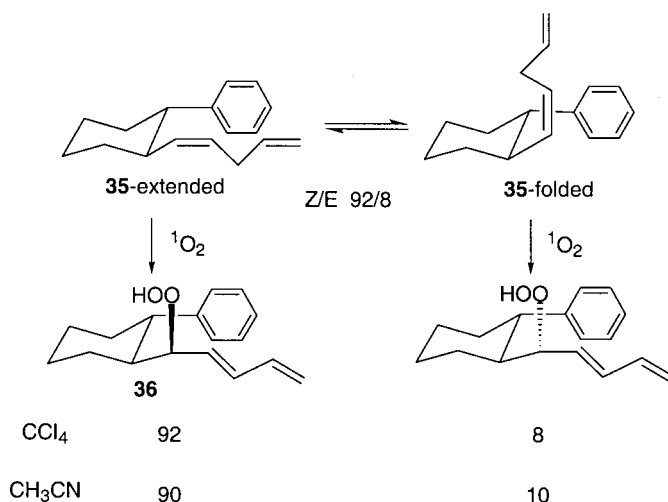
*Case studies.* Dussault and coworkers<sup>65,66</sup> have taken advantage of steric effects to induce diastereoselective peroxidations of 1,4-dienes and enoates. Photooxidation of 1,4-diene **35** occurred with good to very good diastereoselectivity to give 1,3-diene hydroperoxide **36** (Scheme 15) as the predominant product. The formation of **36** is a result of singlet oxygen approach to the sterically accessible face of the more stable extended conformation of 1,4-diene **35**. Consequently, the 2-phenylcyclohexyl group controls both the conformation and the direction of singlet oxygen approach to the diene moiety.



Scheme 13.



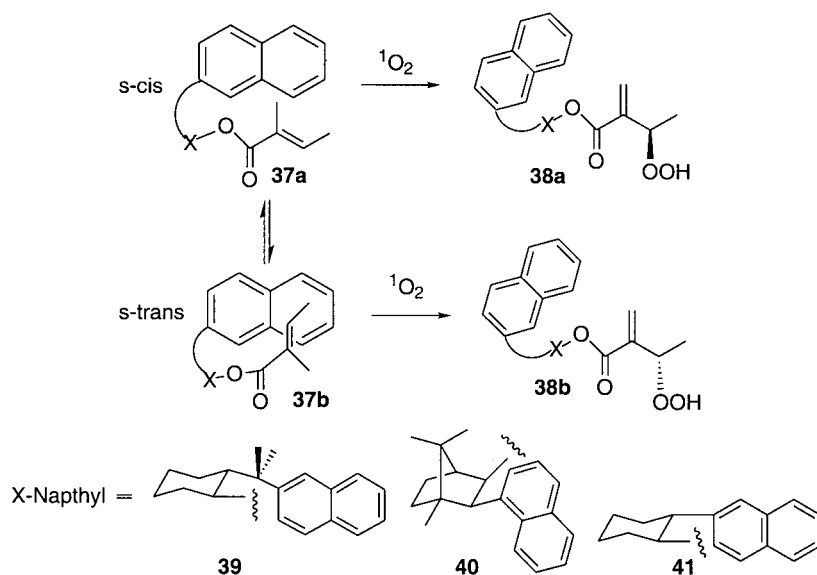
Scheme 14.



Scheme 15.

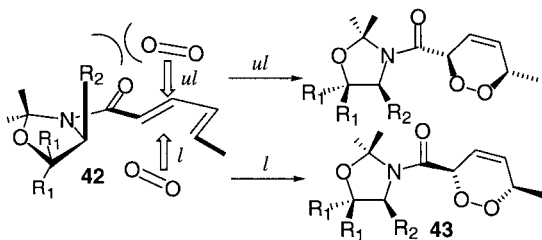
Effective shielding of one stereogenic face of the alkene is a critical feature of these diastereoselective reactions. This is a demanding criterion given the small size of singlet oxygen. For example, acceptable diastereoselective photooxidations of tiglate esters, **37**, were only achieved at

−60°C with the (2-naphthyl)methyl chiral auxiliary **39**. Neither the bicyclic auxiliary **40** nor the (2-naphthyl)cyclohexyl chiral auxiliary **41** was nearly as effective. This was attributed to the inability of either **40** or **41** (Scheme 16) to align the naphthyl group parallel and in close proximity

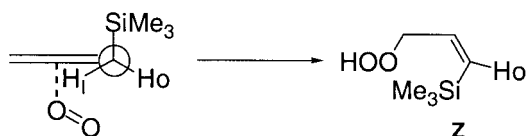


Scheme 16.





Scheme 17.



Scheme 18.

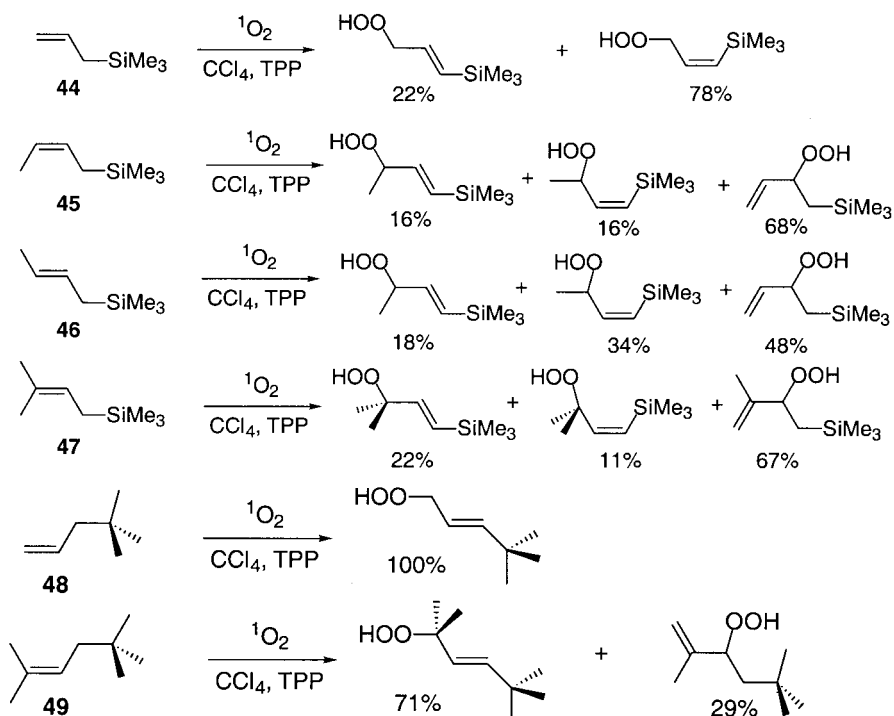
(<4.5Å) to the tiglate ester group. Contrary to expectations, based upon the reported enhanced reactivity of the *s*-isomer,<sup>40</sup> **38b** was the preferred product formed during photooxidations of **39**. Dussault and coworkers<sup>66</sup> have suggested that different populations rather than differing reactivities of the two enolate conformations **37a** and **37b** would explain the results.

Wirth and coworkers<sup>67</sup> have reported the use of optically active 2,2-dimethyloxazolidines, as sterically controlling chiral auxiliaries, in [4+2] cycloadditions of singlet oxygen to a tethered 1,3-diene. Unlike (*ul*) approach of singlet oxygen to **42** encounters severe steric interactions with the R<sub>2</sub> substituent on the oxazolidine and as a consequence like (*l*) attack to give **43** (Scheme 17) is prevalent.

### 3.2. Electronic effects

Electronic effects, in direct analogy to steric effects, can operate at several points on the reaction surface (Scheme 2). For example, electronic interactions can operate in the substrates to bias the conformational equilibrium and dictate which allylic hydrogen is available for abstraction in the ene reaction. The strong propensity of silicon–carbon bonds to hyperconjugatively interact with π-systems produces a preference for a conformation in which the silicon is perpendicular or near perpendicular to the plane containing the double bond<sup>68</sup> (Scheme 18). An *anti*-S<sub>E</sub>2' addition of singlet oxygen would consequently place the terminal oxygen in the peroxide intermediate closer to the inside H<sub>i</sub>, rather than to the outside hydrogen, H<sub>o</sub>, and thereby generate an 'abnormal' preference for the *Z*-allylic hydroperoxide (Scheme 18). This behavior has been documented for several allylic silanes including **44–47**.<sup>69–74</sup> Especially intriguing is a comparison of the photooxidations of allylic silanes **44** and **47** to photooxidations of their hydrocarbon analogues **48** and **49** (Scheme 19). The allylic silanes generate substantial quantities of the *Z*-allylic hydroperoxides while their hydrocarbon analogues react with *E*-stereoselectivity. The slightly smaller effective size of the trimethylsilyl group in comparison to the *tert*-butyl group does not provide a satisfactory explanation for the magnitude of this effect.<sup>74</sup> Hydrogen abstraction from the methyl group competes more effectively with hydrogen abstraction from the methylene α to the trimethylsilyl group in the *cis* alkene, **45**, than in the *trans* alkene, **46**, consistent with the operation of the *cis*-effect (vide supra). The relative reactivities of **45/46** (1.7/1) also supports a contribution from the *cis*-effect in addition to the stereo-electronic effect of the trimethylsilyl group.<sup>74</sup>

Another fascinating example of electronic effects influencing

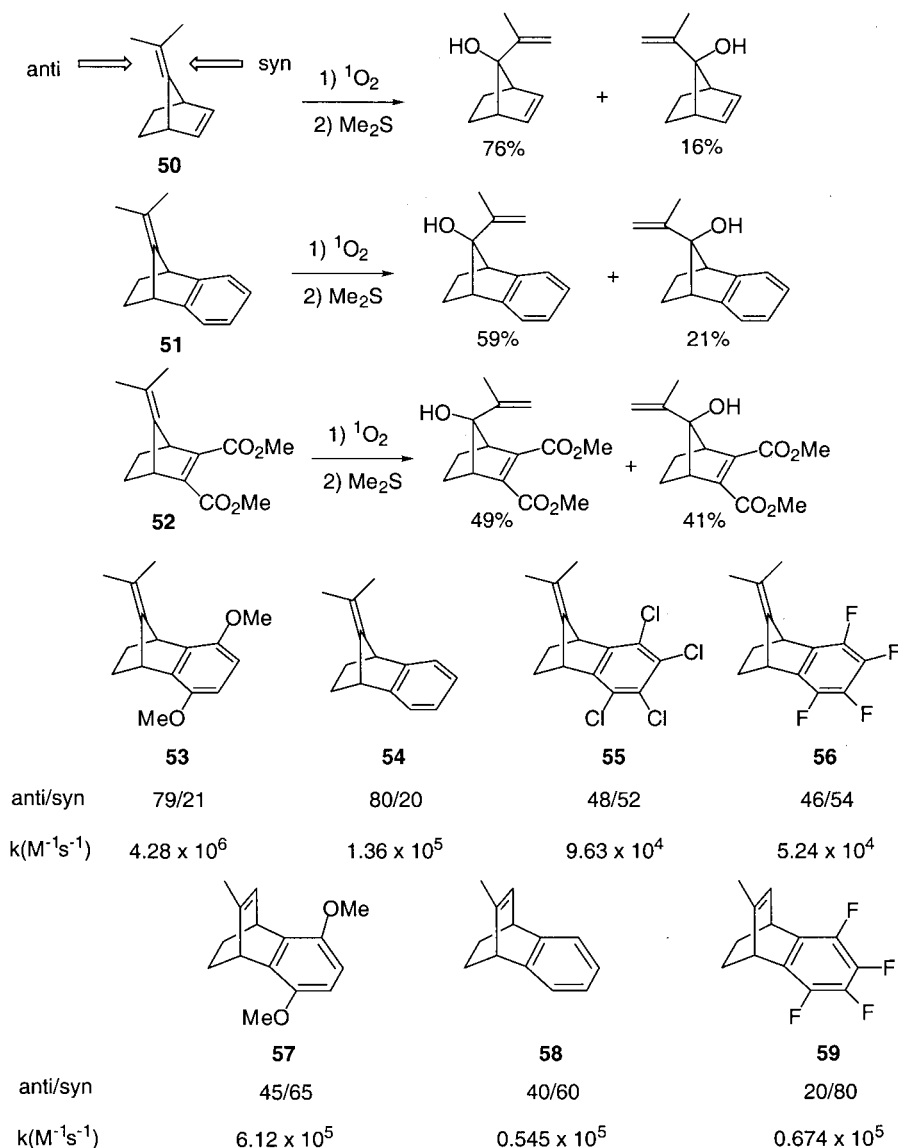


Scheme 19.

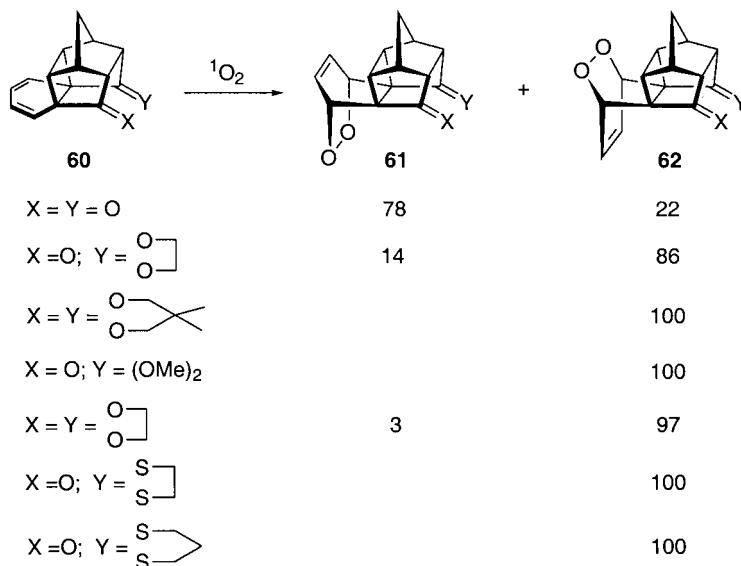
the approach of singlet oxygen to stereogenic faces of an alkene is found in the ene reactions of 7-isopropylidenebornene derivatives. Photooxidations of **50–52** resulted in a preference for contrasteric approach of singlet oxygen to the *anti*-face of the isopropylidene double bond.<sup>75</sup> Paquette and coworkers<sup>76,77</sup> have elegantly demonstrated that the stereoselectivity for addition of singlet oxygen to 7-isopropylidenebenzonorbornenes **53–56** is dramatically influenced by the electron density in the aryl ring. The rate constants for reactions of singlet oxygen with **53–56** span a range of nearly two orders of magnitude.<sup>78</sup> These authors suggest that kinetic effects of this magnitude are consistent with anchimeric  $\pi$ -electron density donation to the developing *anti*-peroxide.<sup>78</sup> They do not feel that  $\pi$ -orbital distortion<sup>75,76</sup> arising from the mixing of the isopropylidene  $\pi$ -orbital with a high lying  $\sigma$ -orbital could be responsible for a kinetic effect of this magnitude. Houk and coworkers<sup>79</sup> however have suggested, as a result of a computational study, that there is nothing special about *anti* addition but rather that *syn* addition is disfavored as a result of electrostatic repulsion between singlet oxygen and the  $\pi$  cloud of

the aromatic ring. The rate constants for photooxygenation of the series of bicyclooctadienes **57–59** (Scheme 20) are less sensitive to changes in the electron density on the aryl ring than were the benzonorbornenes **53–56**.<sup>78</sup> In these substrates the negatively charged pendant oxygen in the developing peroxide points in a direction away from the aryl ring.

Mehta and Uma<sup>80</sup> have recently reported the additions of singlet oxygen to hexacyclo[7.5.1.0<sup>1,6</sup>.0<sup>6,13</sup>.0<sup>8,12</sup>.0<sup>10,14</sup>]penta-deca-2,4-diene-7,15-dione, **60** (X=Y=O), and its derivatives (Scheme 21). Addition of singlet oxygen to the 1,3-diene occurred predominantly from the cyclobutane face to give endoperoxide **62** except in the parent dione, **60** (X=Y=O), in which carbonyl face addition was preferred. The authors suggested that in the oxygen ketals a repulsive interaction between the electron-rich oxygens in the ketal linkages and the incoming singlet oxygen destabilized attack from the ketal face of the diene. On the other hand, the authors suggested that both this electrostatic effect and a Cieplak<sup>81</sup> hyperconjugative orbital effect (Scheme 21)



Scheme 20.



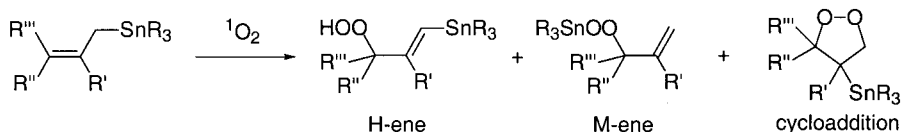
Scheme 21.

were operating cooperatively during additions to the thio-ketal substituted substrates. They based this suggestion on the presumption that electrostatic repulsion alone would not give a greater preference for cyclobutane face attack than that observed for the oxygen analogues. They argue that the electrostatic repulsion should be less in the thioketals than in the oxygen ketals because of the orbital mismatch between the 3p orbitals on sulfur and the 2p orbitals on the approaching singlet oxygen.

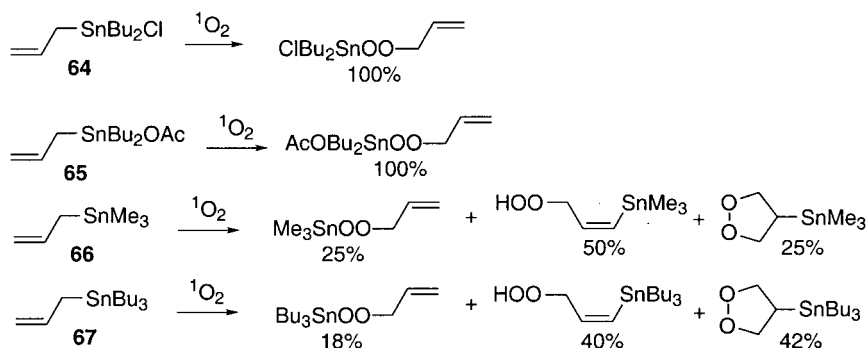
Attractive interactions between singlet oxygen and substituents have also been invoked in order to rationalize product compositions. For instance Dang and Davies<sup>82–85</sup> have reported that addition of singlet oxygen to allylic stannanes can generate three products; a metal ene (M-ene), hydrogen ene (H-ene) and cycloaddition products (Scheme 22). The amount of M-ene product was dramatically enhanced in

allylic stannanes with highly electropositive tin centers consistent with an attractive interaction between the pendant oxygen in the perepoxide and the tin (e.g. compare **64** and **65** to the photooxidations of **66** and **67**) (Scheme 23). The insertion of oxygen into the metal carbon bond in these reactions is accompanied by a shift of the double bond ruling out the possibility that a direct insertion of oxygen is occurring. In addition, these workers also pointed out that there is no evidence for the operation of S<sub>H</sub>2 or S<sub>H</sub>2' (radical) mechanisms to give the M-ene product.

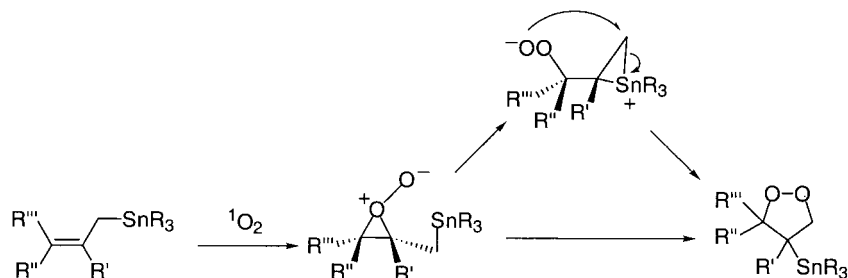
The formation of the 1,2-dioxolanes in the reactions of **66** and **67** are examples of the electronic effect of the tin operating during decomposition of the perepoxide intermediate (Scheme 24). The ability of tin to stabilize β-carbocations and to anchimerically assist their formations via a bridged intermediate (β-effect) is responsible for the



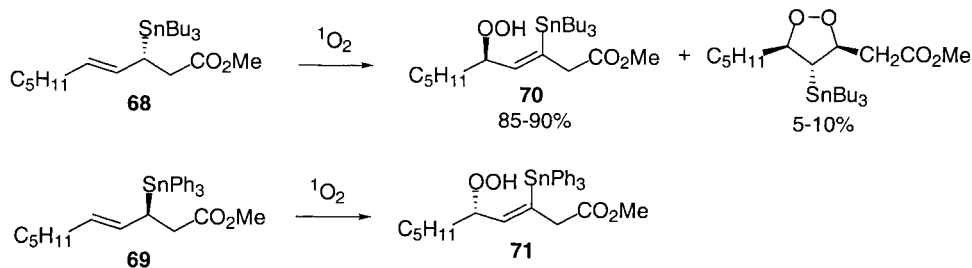
Scheme 22.



Scheme 23.



Scheme 24.



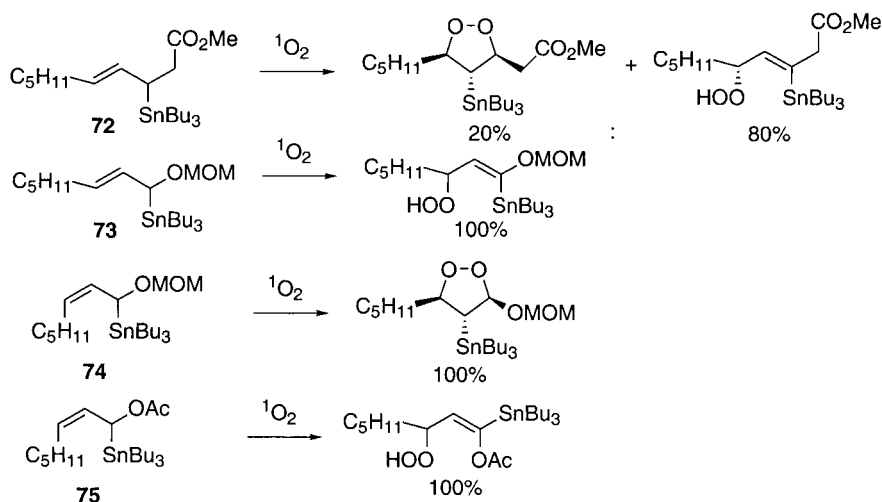
Scheme 25.

formations of the dioxolanes. 1,2-Dioxolanes were not observed during photooxidations of allyl silanes despite the well established, albeit reduced efficiency, of the silicon  $\beta$ -effect.<sup>12,71,72,82</sup>

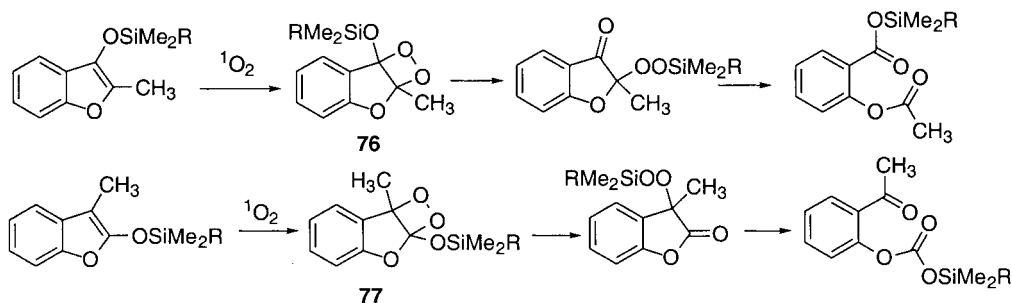
In a series of elegant investigations Dussault and coworkers<sup>66,86</sup> have attempted to improve the synthetic utility of these allylic tin photooxidations. For example, photooxidations of the chiral allylic stannanes **68** and **69** led stereoselectively to allylic hydroperoxides **70** and **71** (Scheme 25). This stereochemical outcome is consistent with an *anti*- $S_E2'$  addition of singlet oxygen to give what appears to be a single polarized peroxide which decomposes by abstraction of the inside hydrogen (Scheme 18) on the tin bearing carbon. The *cis*-stereochemistry of 3,5-substituents on the dioxolane is also consistent with migration of tin in the peroxide intermediate. The absence of dioxolane in the reaction of **69**

reflects the reduced migratory aptitude of the triphenyl group in comparison to the tri-*n*-butyl stannyl group. These photooxidations did not lead to any M-ene product which led to the speculation that the M-ene reaction is less important for allylic stannanes in which the tin is bonded to a 2° rather than a 1° allylic carbon.

$\alpha$ -Alkoxy allylic stannanes<sup>87</sup> have also been examined in anticipation that the alkoxy group would enhance 1,2-dioxolane formation by stabilizing a developing positive charge at the migration origin. However, examination of the product ratios in the photooxidations of allylic stannanes **72–74** reveals that suppression of the competing ene reaction as well as electronic stabilization is necessary to enhance 1,2-dioxolane formation. The ene reaction is suppressed in **74** since allylic strain prevents easy access to the conformation that places the hydrogen on the tin bearing carbon in the proper alignment for abstraction.



Scheme 26.



Scheme 27.

Even in the presence of allylic strain, however, 1,2-dioxolane formation does not occur in **75** (Scheme 26) since the  $-OAc$  group does not provide as much electronic stabilization as the  $-OMOM$  group.

Electronic effects might also operate during decomposition of dioxetanes. Adam and coworkers<sup>88</sup> reported that dioxetanes **76** and **77** (Scheme 27) do not decompose directly to carbonyl compounds but via rearrangement to a trialkylsilyl peroxide followed by Hock–Criegee cleavage. In both cases only the dioxetane C–O bond  $\beta$  to the  $-SiMe_2R$  group is broken.

### 3.3. Hydrogen bonding effects

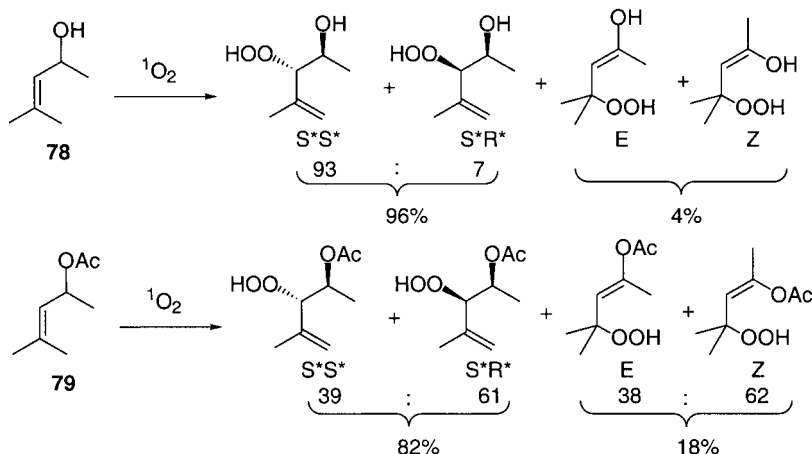
Hydrogen bonding to singlet oxygen can be successfully utilized to control the facial/diastereoselectivity of its ene reactions with acyclic alkenes.<sup>11,89</sup> However, the steering effect of hydrogen bonding must be coupled with a conformational bias for a single conformer of the alkene in order to produce synthetically useful diastereoselectivities.<sup>10</sup> Adam and coworkers have elegantly demonstrated that allylic strain ( $A_{1,3}$  strain) can provide this necessary conformational bias in a series of allylic alcohols<sup>90–92</sup> and amines.<sup>93,94</sup>

The effect of hydrogen bonding can be dramatically illustrated by a comparison of the singlet oxygen ene reactions of allylic alcohol **78** and its acylated derivative **79** (Scheme 28). The allylic alcohol, **78** exhibits a striking diastereoselectivity for the threo ( $S^*S^*$ )  $\beta$ -hydroxy allylic

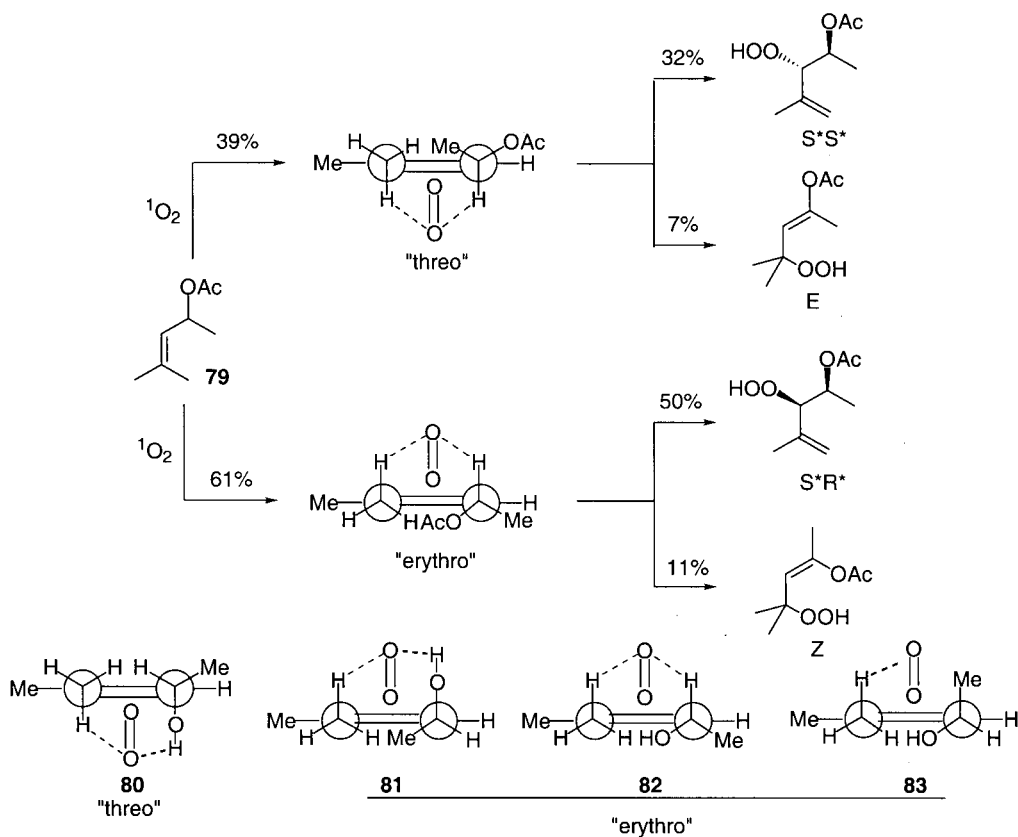
hydroperoxide while its acylated derivative **79** exhibits a modest erythro ( $S^*R^*$ ) diastereoselectivity.

The diastereoselectivity in the photooxidation of the allylic acetate, **79**, is consistent with the operation of the *cis*-effect. (Scheme 29) The ene reaction occurs via threo and erythro perepoxides that both enjoy maximum stabilization by interaction of the pendant (trailing) oxygen with two allylic hydrogens. Consequently, the preference for the erythro product reflects the smaller allylic strain ( $A_{1,3}$  strain) induced by the acetate in comparison to the methyl group. The excellent diastereoselectivity for the threo product during photooxidation of the allylic alcohol, **78**, however, is inconsistent with the operation of the *cis* effect but is consistent with preferential reaction via the hydrogen bonded threo perepoxide, **80**, rather than through the less stable erythro perepoxides, **81**, **82**, or **83**. (Scheme 29) The significant erosion of threo diastereoselectivity during photooxidation of **78** in methanol provides compelling corroboration of its hydrogen bonding origin.<sup>95,96</sup> The precise identity of the perepoxide precursor of the minor erythro product during photooxidation of **78** is not known with certainty, however, it cannot form exclusively via the hydrogen bonded perepoxide **81** since an increase in size of the allylic substituent from methyl to *t*-butyl is not accompanied by an increase in the threo isomer.<sup>91</sup>

The importance of allylic  $A_{1,3}$  strain can be demonstrated by comparison of the *E* and *Z* isomers of allylic alcohol **84**. The *Z* isomer is highly threo diastereoselective while the *E*



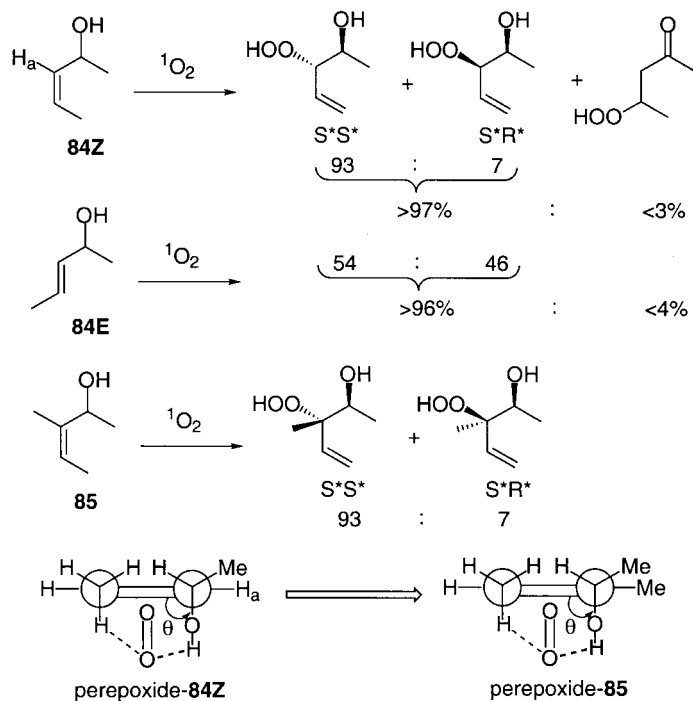
Scheme 28.



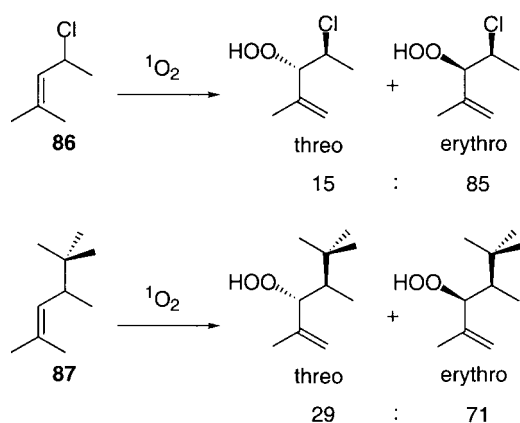
Scheme 29.

isomer, with significantly reduced allylic strain, exhibits dramatically diminished threo diastereoselectivity. On the other hand  $A_{1,2}$  strain does not appear to play any role in determining the stability of the threo perepoxide since replacement of  $H_a$  in **84Z** by a methyl group to give **85**

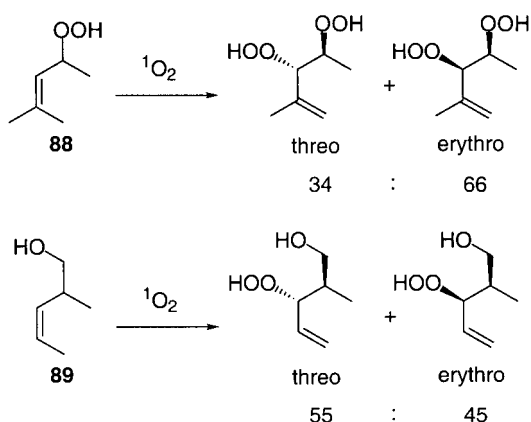
(Scheme 30) has no effect on the threo diastereoselectivity. Adam and Nestler<sup>97</sup> have suggested that the absence of  $A_{1,2}$  strain effect on diastereoselectivity is indicative of an angle  $\theta$  (see perepoxides **84Z** and **85**) of between 90 and 130°.



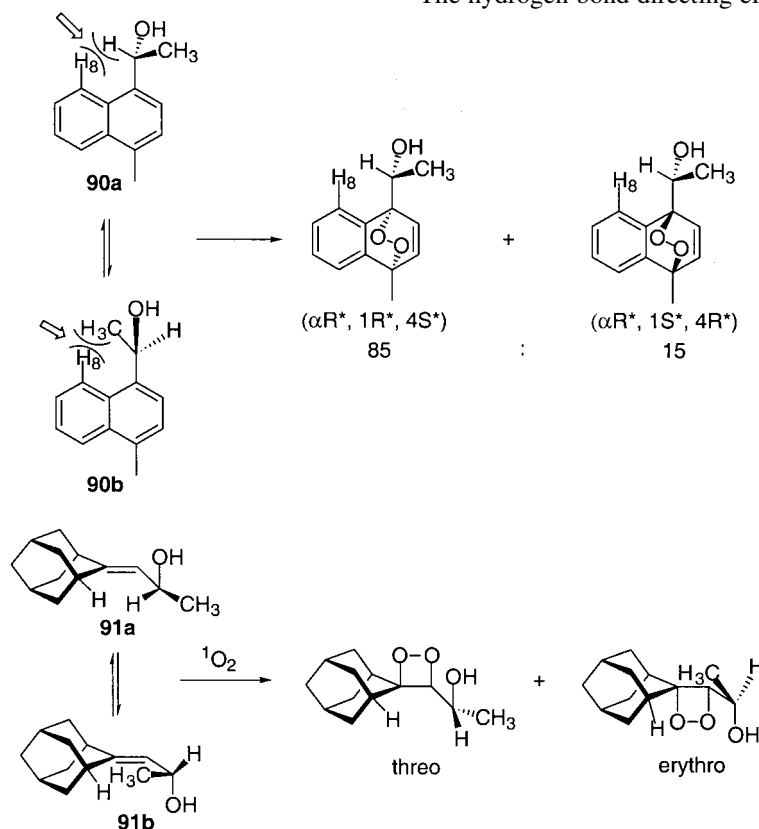
Scheme 30.



Scheme 31.



Scheme 32.

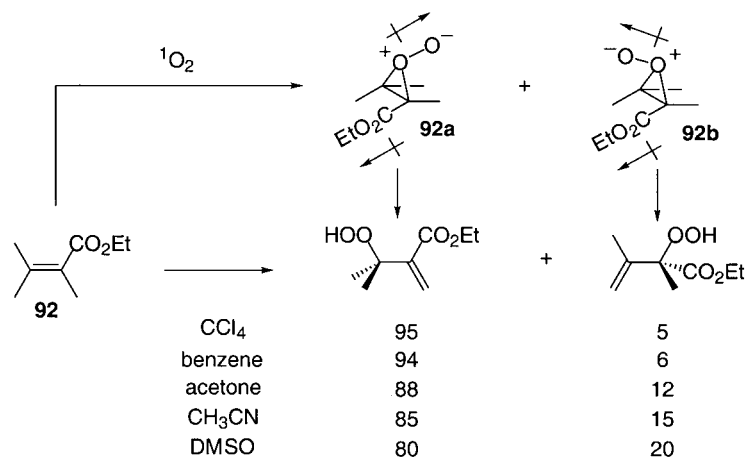


Scheme 33.

Adam and coworkers have examined a large number of allylic substituents and have classified them as either having attractive (hydrogen bonding: OH, NH<sub>2</sub>, NH<sub>3</sub><sup>+</sup>) or repulsive (NHAc, NHBoc, NHPht, NBoc<sub>2</sub>, *t*Bu, Cl) interactions with the pendant oxygen in the perepoxide.<sup>94</sup> The substituents that have attractive (hydrogen bonding) interactions with the perepoxide are threo selective while those that have repulsive interactions are erythro selective. The repulsive interactions can either be steric or electronic<sup>98</sup> in origin as is evident from a comparison of the photooxidations of **86** and **87**.<sup>9</sup> (Scheme 31) The chloride in **86** is more erythro selective than the *tert*-butyl in **87** despite the fact that it is a smaller substituent.

The ability of hydrogen bonding, or for that matter electronic and steric effects, to influence the singlet oxygen ene reaction is understandably a sensitive function of the geometric placement of the substituent relative to the reaction center.<sup>10</sup> For example, the allylic hydroperoxide **88** and the homoallylic alcohol **89** (Scheme 32) react with very poor diastereoselectivity.<sup>9,99</sup> In both cases hydrogen bonding to the perepoxide would generate an unfavorable 7-membered ring. The efficacy of the hydrogen bond steering effect also appears to be related to the nucleophilicity of the alkene. Electron poor olefins react via reversible perepoxide formation and it is the efficiency of hydrogen abstraction in the second step ( $k_2$  in Scheme 2) rather than the hydrogen bond directed formation of the perepoxide that determines reaction regiochemistry. As a result ene reactions of electron poor allylic alcohols are relatively insensitive to solvent effects.<sup>10</sup>

The hydrogen bond directing effect has also been shown to



Scheme 34.

operate during [4+2]<sup>8,100–103</sup> and [2+2]<sup>104</sup> cycloadditions of singlet oxygen. For example, the reduced *peri* strain in **90a** in comparison to **90b** coupled with the hydrogen bond directing effect generates an 85/15 preference for the ( $\alpha R^*$ ,  $1R^*$ ,  $4S^*$ ) diastereomer. The synergistic interaction between allylic strain and the hydroxy directing effect in the adamantylidene allylic alcohol **91** (Scheme 33) leads exclusively to the threo rather than the erythro dioxetane via [2+2] addition of singlet oxygen to the conformationally preferred rotomer **91a**.

#### 4. Environmental Effects

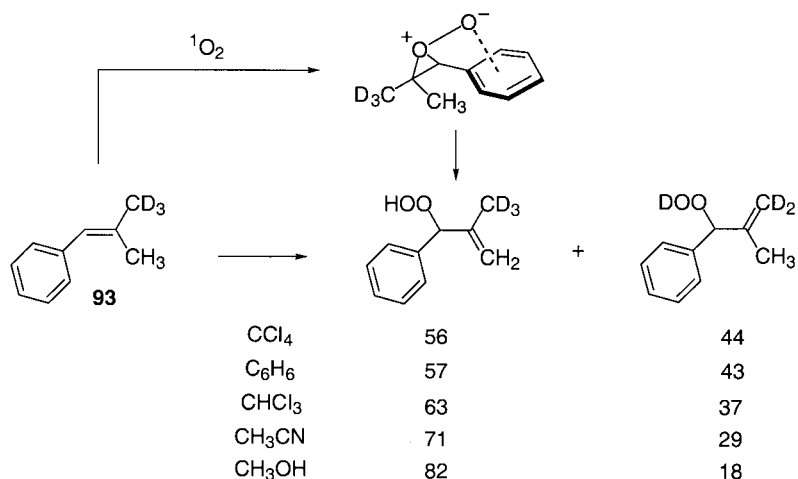
##### 4.1. Solvent effects

In 1984 Gollnick and Griesbeck<sup>105</sup> reported the rate constants for photooxidations of a wide variety of substrates in several different solvents. The rate constants for the singlet oxygen ene and 4+2 cycloadditions were nearly independent of solvent. In stark contrast, the 2+2 cycloadditions showed a dramatic solvent sensitivity. This report is consistent with earlier observations that in reactions where ene and 2+2 cycloadditions compete that the product ratios were very sensitive to solvent polarity.<sup>105,106</sup>

Manring and Foote<sup>107</sup> reported that both the product ratio and the rate constant for the reaction of 2-methyl-2-pentene with singlet oxygen were sensitive to solvent polarity. However, the magnitudes of these solvent effects are small and as a consequence do not provide a generally useful synthetic tool. Orfanopoulos and Stratakis<sup>108</sup> have also reported a solvent effect during photooxidations of the  $\alpha,\beta$ -unsaturated ester **92**. They suggested that the larger dipole moment of piperoxide intermediate **92b** in comparison to **92a** (Scheme 34) was responsible for the observed change in product ratio.

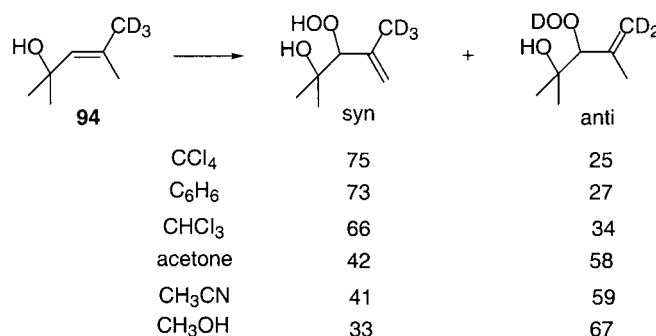
A surprisingly large solvent effect has been reported for the photooxidation of  $\beta,\beta$ -dimethylstyrene, **93**.<sup>109</sup> (Scheme 35) The magnitude of the solvent effect was attributed to an electrostatic interaction between the phenyl ring and the pendant oxygen in the piperoxide that is selectively stabilized in polar solvents.

The largest observed solvent effects, however, appear to be due to solvent interruption of the hydrogen bond steering effect reported by Adam and coworkers<sup>10</sup> (*vide supra*). This was elegantly illustrated by looking at the photooxidation of **94** as a function of solvent.<sup>95</sup> (Scheme 36) The formation of the *syn*-hydroperoxide is significantly diminished in both

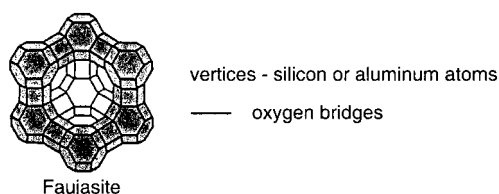


Scheme 35.





Scheme 36.



Scheme 37.

hydrogen bond donating and accepting solvents. Presumably the hydrogen bond donating solvents provide alternative stabilization of the peroxide and hydrogen bond accepting solvents interact with the allylic hydroxyl group preventing internal complexation. In the absence of the hydrogen bond steering effect hydrogen abstraction to give the *anti*-hydroperoxide becomes more competitive.

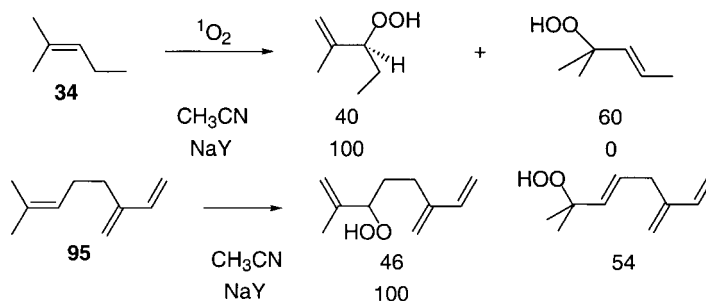
## 4.2. Zeolites

Proven strategies designed to influence the stereo- and regiochemistry of bimolecular reactions often perform poorly in singlet oxygen reactions as a result of its high reactivity and small size. The most successful attempts to improve the diastereo- and enantioselectivity of singlet oxygen reactions have relied on simultaneous control of the substrate conformation and singlet oxygen approach geometry. Consequently, supramolecular systems are very attractive because of their ability to impart 'enzyme-like' organization to the activated complex.

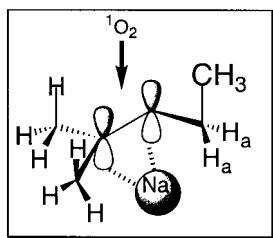
Zeolites are aluminosilicate supramolecular systems consisting of oxygen linked [SiO<sub>4</sub>]<sup>4-</sup> and [AlO<sub>4</sub>]<sup>5-</sup> tetrahedra. Faujasites NaY and NaX (Scheme 37) have attracted considerable attention because of their availability and pore

structure which can easily accommodate organic molecules of interest to the organic chemist.<sup>110</sup> These zeolites have a series of reaction chambers (supercages) which are tetrahedrally connected via windows approximately 7.4 Å in diameter. A negative charge is introduced for each tetrahedral aluminum in the zeolite framework. In order to maintain charge neutrality sodium cations are also located within the zeolite framework.

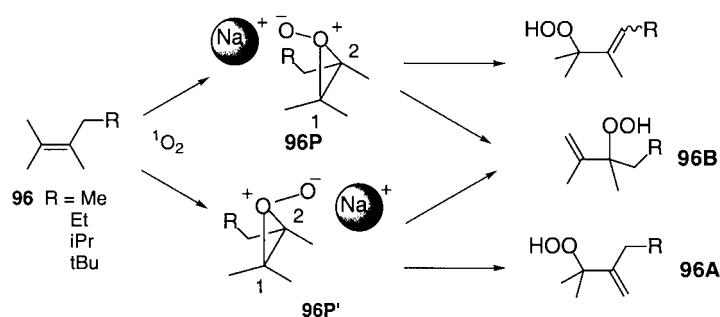
The sodium ions can be easily exchanged for a variety of different cations including cationic sensitizers such as methylene blue.<sup>111</sup> At low doping levels, which insure population of the monomeric sensitizers, excitation at the appropriate wavelength generates synthetically useful quantities of singlet oxygen. Singlet oxygen has been identified in these systems by its characteristic emission at 1268 nm.<sup>112</sup> However, one must proceed with caution since many of the problems associated with photooxidations in homogeneous media are also of concern in the zeolite and one cannot assume that all intrazeolite photooxidations involve singlet oxygen. Type I and Type II photooxidations<sup>113</sup> compete and sensitizer bleaching occurs in intrazeolite photooxidations just as they do in solution. For example, the intrazeolite photooxidations of *trans*-stilbene and *trans*-4,4'-dimethoxy-stilbene cannot be quenched by the singlet oxygen specific quencher, 2,3-dimethyl-2-butene, and probably occur via an electron transfer Type I process.<sup>114</sup> In addition, dye aggregation and acid catalyzed rearrangements of products and/or starting materials can also complicate intrazeolite photooxidations.<sup>115</sup> Consequently, mechanistic conclusions are only valid if it can be shown that the mass balance of the intrazeolite photooxidation is high, if suitable controls to establish the stability's of starting material and products have been conducted, and if tests to distinguish between Type I and II photooxidations have been completed.



Scheme 38.



Scheme 39.



Scheme 40.

In 1996 Li and Ramamurthy<sup>112</sup> reported that intrazeolite photooxidation of 2-methyl-2-pentene, **34**, and  $\beta$ -myrcene, **95** (Scheme 38), were regioselective for a single allylic hydroperoxide product. This is in dramatic contrast to their homogeneous photooxidations that give nearly a 1:1 mixture of two allylic hydroperoxide products. In order to explain this very useful regiochemical change in the zeolite a model was proposed which invoked complexation of the olefin to the sodium cation in the interior of the zeolite (Scheme 39). This interaction serves to anchor the olefin to the framework of the zeolite thereby making only one face of the olefin accessible to the approaching singlet oxygen. In the case of 2-methyl-2-pentene the proximity to the zeolite framework also generates a preferred conformation in which the allylic methyl is forced to occupy the face approached by singlet oxygen (Scheme 39). Consequently, the allylic hydrogens on the ethyl group ( $H_a$ ) are not accessible and hydrogen abstraction occurs exclusively on the *gem*-dimethyl end of the double bond.<sup>116</sup> In 1998 Ramamurthy and coworkers<sup>117</sup> suggested a second tentative model to explain the intrazeolite photooxidations. In this new model the cation serves to polarize the double bond to place the greatest amount of positive charge on the *gem*-disubstituted end of the olefin directing oxygen to the least substituted end of the olefin.

In 1999 the intrazeolite photooxidations of a series of tetra-substituted alkenes, **96**, were reported.<sup>118</sup> The ene regio-chemistries of **96** in solution were very sensitive to the size of the allylic substituent R. As the size of R increased from Me- to *t*Bu- the proximal C<sub>2</sub>-O bond in perepoxides **96P** and **96P'** (See Scheme 40 for the sodium complexed form of these perepoxides) lengthen and weaken inducing cleavage and predominant hydrogen abstraction from the methyl group geminal to the substituent to give increasing amounts of **96A**. If a model similar to that shown in Scheme 39 operates, the steric effect of the allylic substituent should

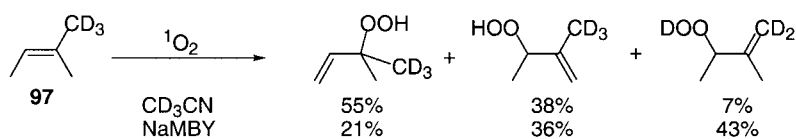
be amplified in the zeolite and an increase in hydrogen abstraction from the methyl geminal to the substituent should be observed. Examination of Table 2 reveals that indeed the **96A/96B** ratio increases in the zeolite sodium methylene blue Y (NaMBY) in comparison to solution for R=Me and R=Et.<sup>119</sup> However, the ratio is approximately the same for R=*i*Pr and is significantly smaller than in CH<sub>3</sub>CN when R=*t*Bu. These results require a significant modification of the model depicted in Scheme 39.

The results depicted in Table 2 can be explained if complexation of the sodium with the pendant oxygen in the perepoxide rather than with the double bond as shown in Scheme 39 were the regiochemically important interaction (Scheme 40). In this new model the interaction of the sodium with the pendant oxygen in the perepoxide would place more positive charge on the carbon framework. Consequently, Markovnikov directing effects should be more important in the zeolite than in solution. In addition, the steric interaction between the sodium and the substituents on the perepoxide rather than the *cis* effect will determine the relative energies of **96P** and **96P'**.

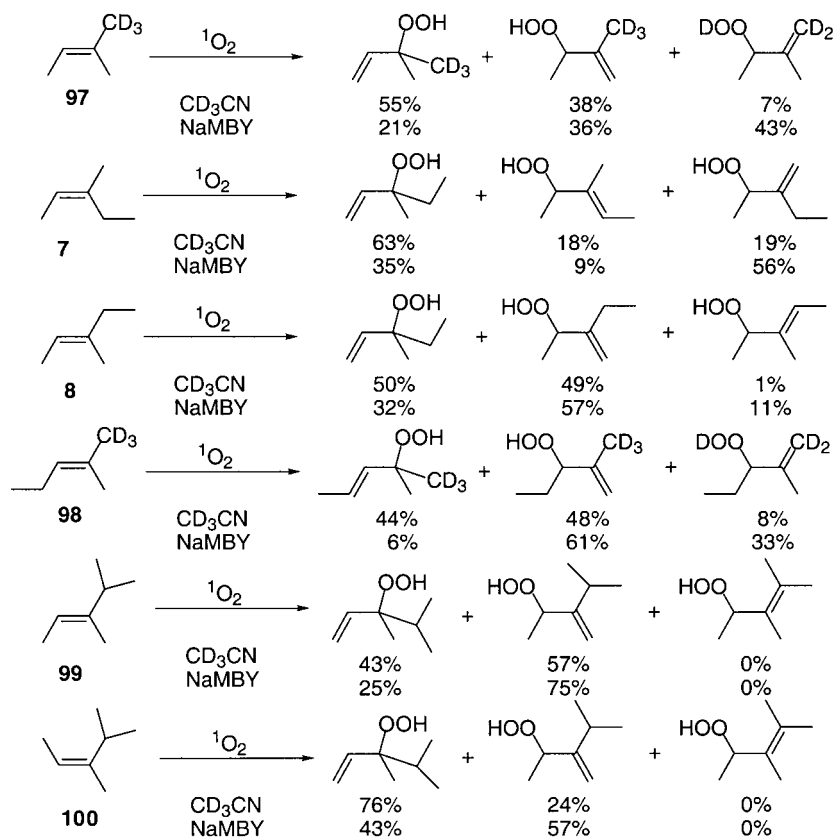
Several other experimental observations were reported to support this new model. These included: (1) the isotope effect ( $k_H/k_D$ ) for the photooxidation of *Z*-2,3-dimethyl-1,1,1,4,4,4-hexadeutero-2-butene, **14Zd<sub>6</sub>** was  $1.04 \pm 0.02$ . This is consistent with a perepoxide intermediate rather than an open zwitterion. (2) the '*cis* effect' is less important during the photooxidation of **97** (Scheme 41) in NaMBY than in solution consistent with the steric interaction implicit in the model in Scheme 40 and discussed

**Table 2.** A comparison of solution and zeolite (NaMBY) photooxidations of alkenes **96**

R	Solution			Zeolite		
	%96A	%96B	96A/96B	%96A	%96B	96A/96B
	Me	32.9±3.3	67.1±3.3	0.49	39.5±3.7	60.5±3.7
Et	42.0±1.7	58.0±1.7	0.72	52.7±1.7	47.3±1.7	1.11
<i>i</i> Pr	52.6±1.1	47.4±1.1	1.1	51.8±2.8	48.2±2.8	1.07
<i>t</i> Bu	70.6±1.1	29.4±1.1	2.4	61.2±1.1	38.8±1.1	1.58



Scheme 41.



Scheme 42.

above,<sup>120</sup> and (3) substituent effects as detected by a Hammett substituent effect study are more important in the zeolite than in solution consistent with a greater positive charge on the carbon framework of the peroxide.

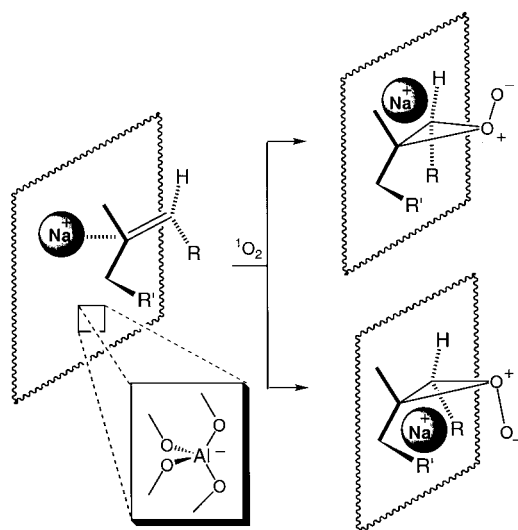
Stratakis and Froudakis also reported that the *cis* effect was less important in intrazeolite photooxidations than in solution consistent with the model in Scheme 40.<sup>121</sup> They also suggested a model which invoked both interaction of the sodium cation with the alkene as shown in Scheme 39 and with the peroxide as shown in Scheme 40. They made the interesting suggestion that unsymmetrical complexation of the sodium with the alkene placed the cation on the less hindered side of the alkene favoring formation of the less hindered peroxide. No experimental data, however, were reported which required that the alkene/sodium complex be on the reaction surface for hydroperoxide formation. Consequently, the possibility that a small amount of free alkene in equilibrium with the alkene/sodium complex is the species that reacts with singlet oxygen cannot be ruled out. However, Cleman and Sram during a study of a series of trisubstituted alkenes, **7**, **8**, and **97–100** (Scheme 42), provided the first experimental evidence which required

that both complexation of sodium to the alkene and to the peroxide play a role in determining the ene regioselectivity.<sup>122</sup>

Of particular interest is the *gem/trans* ratio of hydrogen abstraction from the most highly substituted side of trisubstituted alkenes (Table 3). This ratio is a measure of the end selectivity (Markovnikov directing effect) for

Table 3. End selectivity on the most congested side of the alkene

Compound	<i>gem/trans</i>	
	CH <sub>3</sub> CN	Zeolite
<b>97</b>	0.69	1.71
<b>8</b>	0.98	1.78
<b>7</b>	0.29	0.26
<b>98</b>	1.09	10.2
<b>99</b>	1.33	3.0



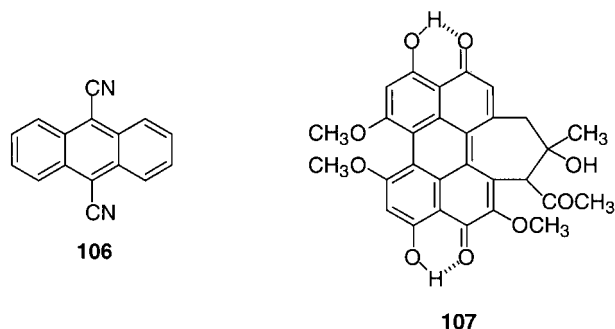
Scheme 43.

hydrogen abstraction by the peroxides formed on the more congested side of the olefin. This end selectivity (*gem/trans*) changes from 0.69 to 1.71 in **97**, from 0.98 to 1.78 in **8**, and from 1.33 to 3.0 in **99** as the reaction medium is changed from  $\text{CD}_3\text{CN}$  to NaMBY. Consequently, Markovnikov directing effects are more important in the zeolite than in solution. The magnitudes of the increases in the Markovnikov directing effects for all trialkyl substituted alkenes should be similar to those observed for **97**, **8**, and **99** since alkyl groups all have similar inductive characters ( $\sigma_1$  for Me, Et, and *i*Pr are  $-0.04$ ,  $-0.05$ , and  $-0.06$ , respectively) and should support the same charge distribution on the two  $\text{sp}^2$  alkene carbons. However, the *gem/trans* ratio in **7** and **98** do not conform to that expectation. In both cases there is less hydrogen abstraction at the ethyl group than anticipated based upon the expected Markovnikov selectivity. Rather than seeing an increase in the *gem/trans* ratio of approximately 2–3 it actually decreases from 0.29 to 0.26 in **7** and increases from 1.09 to 10.2 in **98**.

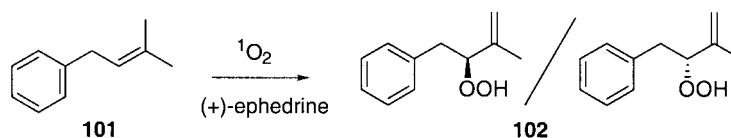
The dramatic decreases in the anticipated abstraction from the ethyl groups in **7** and **98** are most easily rationalized by the model shown in Scheme 43. In this model as singlet oxygen approaches the sodium complexed alkene the sodium migrates to a position which allows a favorable electrostatic interaction with both the pendant oxygen in the peroxide and the negatively charged aluminum in the zeolite framework. The proximity to the wall of the supercage enhances the likelihood of singlet oxygen approach to the face of the olefin occupied by the allylic substituent thereby decreasing the amount of hydrogen abstraction from the ethyl groups in **7** and in **98**.

Attempts to conduct intrazeolite enantioselective photooxidations are limited both in scope and in success.<sup>123,124</sup> Joy and coworkers<sup>125</sup> reported that irradiation of NaY containing the sensitizer thionin and trisubstituted alkene **101** doped with (+)-ephedrine hydrochloride resulted in completely regioselective and modestly enantioselective ( $\sim 15\%$  e.e.) formation of hydroperoxide **102** (Scheme 44). Although this result is not spectacular it is encouraging and suggests that further studies of enantioselective intrazeolite reactions are warranted.

Tung and coworkers<sup>126</sup> have examined the intrazeolite photooxidations of *trans,trans*-1,4-diphenyl-1,3-butadiene, **103**, *trans*-stilbene, **104**, and 2,3-dihydro- $\gamma$ -pyran, **105**, in the pentasil zeolite ZSM-5 using both 9, 10-dicyanoanthracene, **106**, and hypocrellin A, **107**, as sensitizers. ZSM-5 is characterized by two perpendicular pore systems; a circular zig-zag (sinusoidal) channel with a cross section approximately 5.5 Å in diameter and a straight elliptical channel with dimensions of approximately 5.2 Å $\times$ 5.8 Å. These channels are too small to incorporate either sensitizer **106** or **107** but easily accommodate the substrates. Consequently, electron transfer photooxidations that require close approach of the sensitizer and substrate do not compete with singlet oxygen induced photooxidations which can easily occur by diffusion of singlet oxygen into the pore structure of ZSM-5.<sup>127</sup>



*trans,trans*-1,4-Diphenyl-1,3-butadiene, **103**, reacts in solution, using either **106** or **107** as the sensitizer, to give, via dioxetane decomposition, benzaldehyde and *trans*-cinnamaldehyde as the major products. These products were formed via reaction of the butadiene radical cation with superoxide using **106** and **107** as shuttles to remove an electron from **103** (Scheme 45) and to deliver it to oxygen. The same reaction in either dry **106** or **107** doped ZSM-5 (Si/Al=55 and 25) produced exclusively the singlet-oxygen/endoperoxide product. This is consistent with the observation that the cisoid conformation of **103**, with a width of 5.1 Å, is more easily accommodated than its transoid conformation (width 5.5 Å) in the internal void space of the zeolite.



Scheme 44.

	solution		zeolite	
	<b>106</b>	<b>107</b>	<b>106</b>	<b>107</b>
		73	53	0
73	53	0	0	
16	16	0	0	
4	4	0	0	
4	14	0	0	
3	13	100	100	

Scheme 45.

The product composition from photooxidation of *trans*-stilbene, **104** (Scheme 46), is remarkably dependent on reaction conditions. Benzaldehyde is the major product in the solvent pentaerythritol trimethyl ether (PTE) using **106** as the sensitizer. A bis-endoperoxide, however, becomes the major product under identical reaction conditions when **107** is used as the sensitizer. On the other

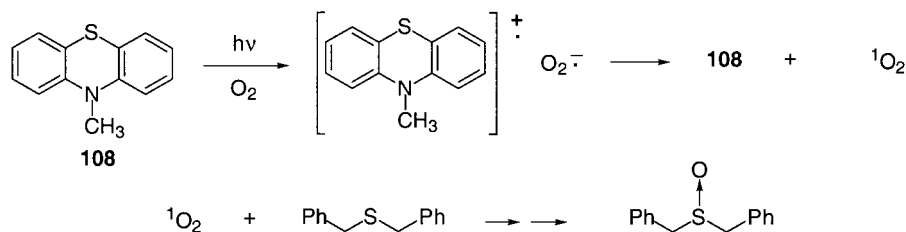
hand, using either sensitizer doped in ZSM-5 produced benzaldehyde as the exclusive product. Consequently, benzaldehyde must be a singlet oxygen derived product via decomposition of the dioxetane in ZSM-5 since electron transfer reactions are precluded under these reaction conditions (*vide supra*). The absence of the bis-*endo*-peroxide, which is also a likely singlet oxygen derived

	solution		zeolite	
	<b>106</b>	<b>107</b>	<b>106</b>	<b>107</b>
		48	3	100
12	0	0	0	
28	0	0	0	
12	0	0	0	
0	97	0	0	

Scheme 46.

	solution		zeolite	
	isooctane	PTE	Si/Al = 55	25
		10	58	40
90	42	60	52	

Scheme 47.



Scheme 48.

product, is probably due to the limited space available in the zeolite channels.

The solution photooxidation of 2,3-dihydro- $\gamma$ -pyran, **105** (Scheme 47), is known to give both dioxetane and ene derived products in solvent polarity dependent ratios, with increasing solvent polarity enhancing dioxetane formation.<sup>128,129</sup> This product ratio is greater in dry ZSM-5 than in isoctane but less than that observed in pentaerythritol trimethyl ether (PTE). This suggests that the reaction in the zeolite occurs near the hydrophilic cation sites. However, since the product ratio is smaller than observed in PTE despite the greater polarity in the vicinity of the cations, it also suggests that other factors besides polarity influences the intrazeolite photooxidation.

Consistent with the importance of cation-alkene interaction during the intrazeolite photooxidations of **103**, **104**, and **105** is the fact that water with its greater affinity for the hydrophilic cationic sites dramatically influences the product ratios. Water appears to displace the alkene to a hydrophobic region of the zeolite or, if the hydrophobic region is too small to accommodate the alkene, to the external surface of the particle.

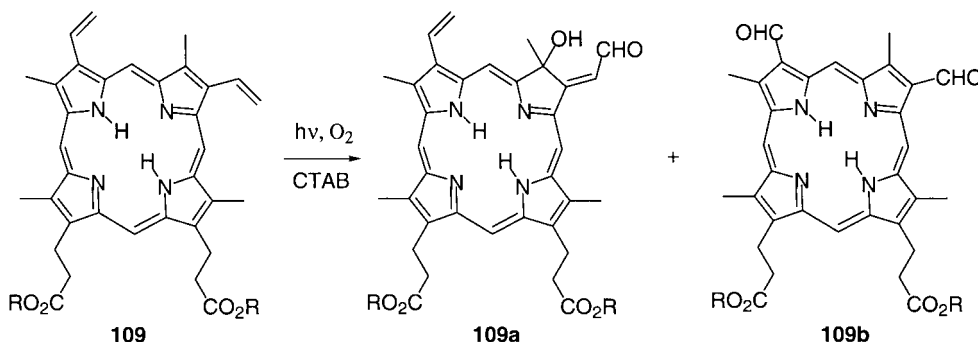
### 4.3. Micelles, vesicles, and microheterogeneous biological structures

Singlet oxygen reactions in aqueous micellar media have been extensively examined.<sup>130</sup> Interest in singlet oxygen reactions in microheterogeneous media have been driven by its similarity to the environment encountered at the cellular level.<sup>131</sup> A recent review article has examined the kinetic behavior of these singlet oxygen reactions and the information it provides on the mobility and location of singlet oxygen and its substrate in and between the different domains provided by these microheterogeneous systems.<sup>132</sup>

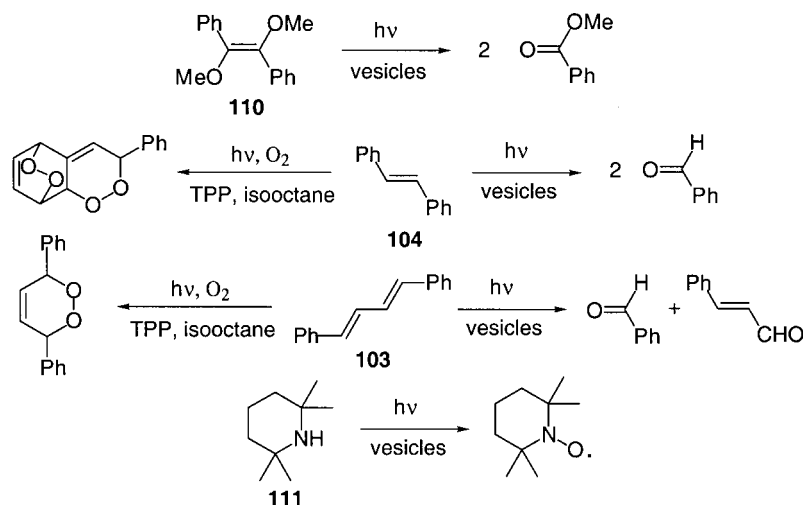
Unfortunately, far fewer studies have examined if the order imposed by these environments can be used to productively influence the yield and/or the stereo- and regiochemistry of singlet oxygen reactions.

In 1982 Hovey<sup>133</sup> reported that irradiation of an aqueous aerated mixture of 10-methylphenothiazine, **108**, in sodium dodecylsulfate (NaDODSO<sub>4</sub>) micelles generated a deep red color which was identified as the radical cation **108**<sup>•+</sup> by ESR. When benzyl sulfide was included in this micellar solution a good to very good yield of benzyl sulfoxide was isolated. It was suggested that electron transfer from excited **108** to triplet oxygen occurred to generate the radical cation superoxide ion pair. A small fraction of the superoxide escapes from the micelle prior to back electron transfer. The negatively charged skin of the micelle then prevents reentry of the superoxide providing kinetic protection to the radical cation. The majority of the ion pair, however, suffers back electron transfer to generate singlet oxygen that ultimately reacts with benzyl sulfide to produce benzyl sulfoxide. Evidence for the involvement of singlet oxygen was generated by observing formation of 2,3-dimethyl-3-hydroperoxy-1-butene when tetramethylethylene was included in the reaction mixture. The reaction also occurs in homogeneous solution but is contaminated with many byproducts including those from the degradation of **108** (Scheme 48).

In 1978 Horsey and Whitten<sup>134</sup> compared the photooxidations of the bis(dihydrocholesterol) ester of protoporphyrin IX, **109**, in solution, in monolayer films, and in micelles. They discovered that the hydroxyaldehyde, **109a**, which presumably is derived from decomposition of the endoperoxide, and the dioxetane derived product, **109b** (Scheme 49), ratio in organized media is much smaller than observed in solution. They attributed the decrease in 4+2 cycloaddition to a greater difficulty to achieve the



Scheme 49.



Scheme 50.

required *s-cis* conformation in organized media presumably as a result of an increase in effective viscosity and to aggregation in the films and micelles. On the other hand, Ohtani et al.<sup>135</sup> reported no difference in product ratios from photooxidation of methyl linoleate in solution and in aqueous emulsion.

Photooxidations of *trans*-1,2-dimethoxystilbene, **110**, *trans*-stilbene, **104**, *trans,trans*-1,4-diphenyl-1,3-butadiene, **103**, and 2,2,6,6-tetramethyl piperidine, **111**, have been examined in a mixed vesicle constructed from equimolar mixtures of the cationic surfactant, octyltrimethylammonium bromide, and the anionic surfactant, sodium laurate. The photooxidations were conducted by mixing these substrate containing vesicles with a separate set of vesicles containing the sensitizers tetraphenylporphyrin (TPP) or methylene blue (MB). Control studies demonstrated that intervesicular exchange did not occur.

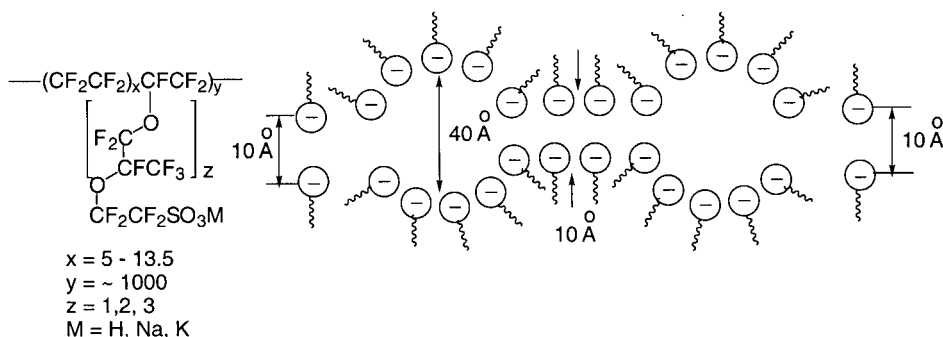
Photooxidations of all four substrates were successful demonstrating that singlet oxygen is capable of diffusing out of the vesicle containing the sensitizer and diffusing into the vesicle containing the substrate. This migration is feasible since the average intervesicle distance is approximately 134 nm, much smaller than the estimated diffusion length of singlet oxygen in H<sub>2</sub>O (780 nm) or in D<sub>2</sub>O (2500 nm). However, the two different vesicle encapsulated sensitizers exhibited different efficiencies since the hydro-

phobic sensitizer TPP generates singlet oxygen in the bilayer membrane while the water soluble MB generates singlet oxygen in the aqueous inner compartment of the vesicle.

In **103**, **104**, and **110** (Scheme 50), the only reaction observed was 2+2 cycloaddition to give a dioxetane which cleaved under the reaction conditions to produce carbonyl containing products. This represents a departure, in the cases of *trans*-stilbene, **104**, and *trans,trans*-1,4-diphenyl-1,3-butadiene, **103**, from the TPP sensitized solution photooxidations which gave the 4+2 cycloadducts. This deviation was explained by the difficulty to achieve the necessary *s-cis* conformation in the organized medium.

#### 4.4. Nafion membranes

In 1984 Lee and Rodgers<sup>136</sup> published a manuscript describing a kinetic study of singlet oxygen in the polymer Nafion. Nafion is a perfluorinated polymer characterized by short appended chains terminated by a sulfonic acid group (Scheme 51). It has the novel and unique property of swelling in water to form cavities approximately 40 Å in diameter connected by 10 Å diameter channels and is often compared to an inverse micelle. Swollen Nafion can absorb and encapsulate aromatic and aliphatic hydrocarbons as well as organic dyes. It is available in several cation exchanged forms such as sodium, potassium, and the parent



Scheme 51.

protonated sulfonic acid form. Lee and Rogers<sup>136</sup> used 2-acetonaphthone photosensitization to generate singlet oxygen in H<sub>2</sub>O, D<sub>2</sub>O, and methanol swollen Nafion as well as in air-dried, and vacuum dried powders. The singlet oxygen was identified by its characteristic infrared emission at 1270 nm. The time resolved emission exhibited mono-exponential decay consistent with rapid exchange between the two major microheterogeneous environments, the aqueous pools and perfluorinated backbone. This was verified by demonstrating that the lifetime of singlet oxygen in the Nafion polymer was intermediate between that observed in water (4 μs) and fluorocarbons (0.59 to 9.4 ms). The measured lifetimes of 55 μs in water-swollen and 270 μs in D<sub>2</sub>O-swollen Nafion were used to suggest that singlet oxygen is 5-times more soluble in the fluorocarbon backbone than in the water cavities. These lifetimes allow for diffusion of singlet oxygen to many water and fluorocarbon regions prior to its decay.

Niu et al.<sup>137</sup> examined the methylene blue photooxidations of anthracene, 9,10-diphenylanthracene, and 2-dimethylaminonaphthalene in Nafion and, for comparison, in ethanol. Their results suggested that the aromatic hydrocarbons are located in the nonpolar backbone region and that the reactions were faster in Nafion than in ethanol. The 1.6 times faster photooxidation in D<sub>2</sub>O than in H<sub>2</sub>O provided confirmation of a Type II (singlet oxygen) reaction.

Tung and Guan<sup>138</sup> in 1998 examined the 9, 10-dicyanoanthracene (DCA), **106**, sensitized photooxidations of *trans*-stilbene, **104**, *trans,trans*-1,4-diphenyl-1,3-butadiene, **103**, and α-pinene, **112** (Scheme 52) in Nafion membranes. They examined the photooxidations of these compounds in Nafion with the sensitizer either embedded in the polymer matrix with the substrate, or physically isolated from the substrate in CH<sub>2</sub>Cl<sub>2</sub> which cannot swell Nafion, thereby effectively preventing diffusion of the sensitizer into the polymer. They compared the photooxidations under these two heterogeneous conditions to the homogeneous photooxidations in methylene chloride (column B in Scheme 52) and in acetonitrile (column A in Scheme 52). They discovered that photooxidations of the substrates in sensitizer doped Nafion enhanced electron transfer initiated photo-

oxidations with the exclusion of a singlet oxygen mediated pathway. On the other hand, in photooxidations where the sensitizer was physically prohibited from approaching the Nafion embedded substrate only singlet oxygen reactions were observed. In homogeneous photooxidations both pathways were observed.

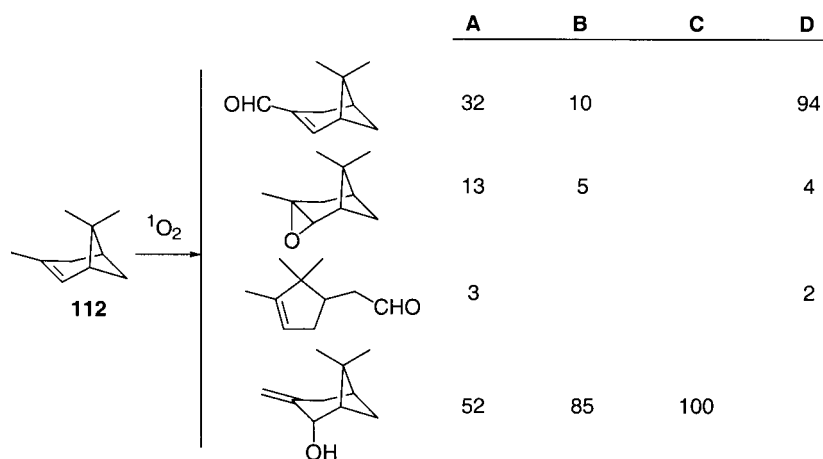
The preference for the electron transfer pathway in the substrate/sensitizer embedded Nafion (column D in Scheme 52) was attributed to the confinement of the substrate and sensitizer in the restricted space of the polymer. Under these conditions the large effective concentrations of the sensitizer and substrates enhanced electron transfer to give the substrate radical cations which subsequently react with superoxide which is formed by donation of an electron to oxygen from the reduced sensitizer.<sup>139</sup>

The exclusive formation of singlet oxygen products under the reaction conditions which physically prevent close approach of the sensitizer to the substrate (column C in Scheme 52) is consistent with the fact that dicyanoanthracene is also capable of sensitizing the formation of singlet oxygen. The 100 μs lifetime of singlet oxygen in methylene chloride<sup>140</sup> and the measured lifetimes in Nafion (*vide supra*) provides more than adequate time for diffusion into the polymer and reaction with the encapsulated substrates under these conditions.

#### 4.5. Miscellaneous efforts to improve regio- and/or stereoselectivity

Stereoselective allylic hydroperoxide formation has also been attempted, with little or only moderate success, using chiral singlet oxygen precursors<sup>141</sup> and photooxidations within chiral inclusion complexes.<sup>142</sup>

Kuroda and coworkers<sup>143</sup> pointed out that in hemoproteins the porphyrin is bound in the hydrophobic pocket of a protein. They also recognized that co-binding of a substrate in the chiral pocket of the protein might significantly effect the reactivity and interactions of the substrate with the porphyrin or with singlet oxygen produced by sensitization.<sup>144</sup> To evaluate this possibility they examined the photooxidations of linoleic acid, **113**, using the tetrakis(*p*-



Scheme 52.



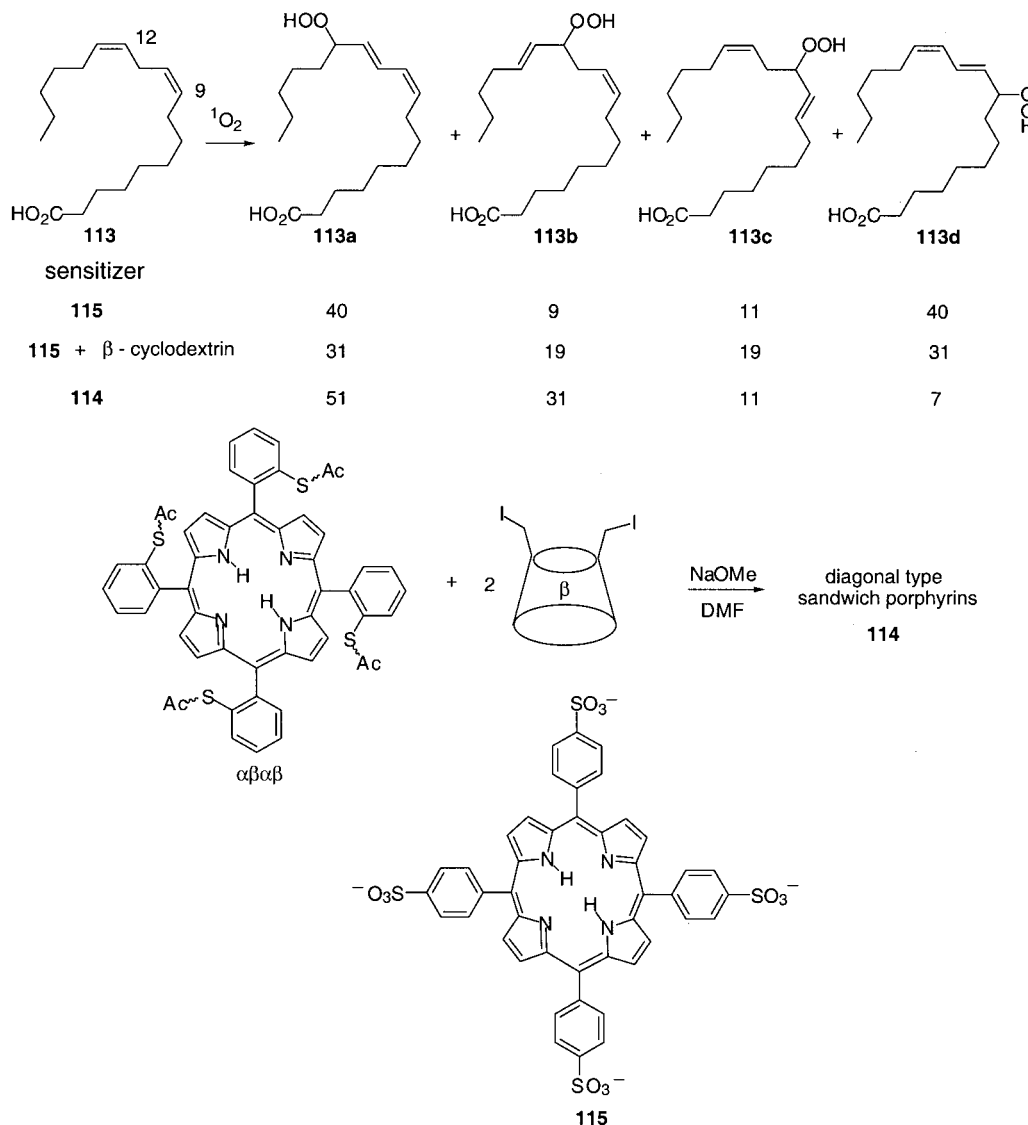
sulfonatophenyl)porphyrin **115** (Scheme 53) in the presence and absence of  $\beta$ -cyclodextrin. They compared these results to the photooxidation with a hemoprotein mimic, a porphyrin covalently sandwiched between two  $\beta$ -cyclodextrins. The sandwich porphyrins **114** used in this study (a 1:1 ratio of two isomers) were made by coupling the  $\alpha\beta\alpha\beta$  atropisomer of tetrakis(*o*-thioacetoxylphenyl)porphyrin with A, D-diiodo- $\beta$ -cyclodextrin.

The  $\Delta^{9,10}$  and  $\Delta^{12,13}$  double bonds in linoleic acid are equally reactive towards singlet oxygen produced by sensitization with **115** in the presence or absence of  $\beta$ -cyclodextrin. However, the ene reaction, using the sandwiched porphyrins **114** as sensitizers occurred preferentially at the  $\Delta^{12,13}$  double bond giving a [**113a**+**113b**]/[**113c**+**113d**] ratio of 82/18. In addition, **113a** and **113b** are formed with significant enantiomeric excesses of 20 and 12%, respectively. Consequently, ene reaction in the hydrophobic pocket of **114** allows control of both regiochemistry and stereogenic face selectivity of singlet oxygen attack.

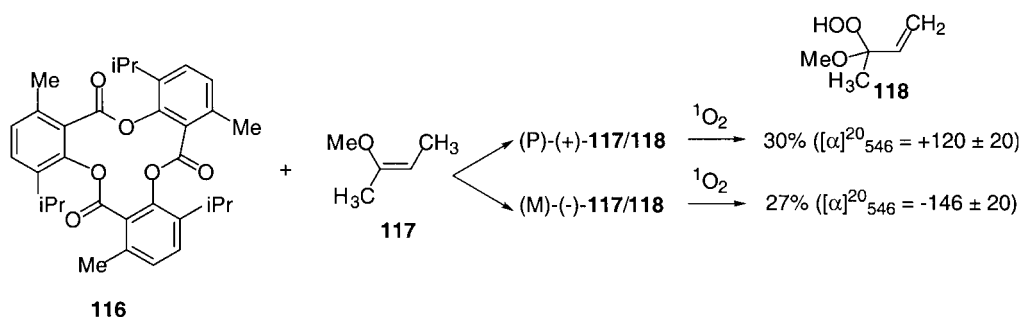
Tri-*o*-thymidine, **116**, exists in solution as rapidly inter-

converting chiral left-handed (M) and right handed (P) conformations. Co-crystallization with enol ether **117** generates a 2/1 (**116**/**117**) clathrate with spontaneous resolution to form crystals consisting entirely of **116** in the M or P configuration.<sup>145</sup> Mechanical separation of the crystals and aerobic irradiation of an intimately mixed powder consisting of either the M or P clathrate and ion resin exchanged bound Rose Bengal resulted in formation of allylic hydroperoxide **118**.<sup>145</sup> (Scheme 54) Examination by polarimetry showed a specific rotation, ( $[\alpha]_{546}^{20}$ ), of  $+120 \pm 20$  and  $-146 \pm 20^\circ$  for the allylic hydroperoxides formed from the (P)-(+)- and (M)-(-)- clathrates, respectively. Singlet oxygen permeates the crystal to react with the clathrate by diastereomeric transition states. Unfortunately, the optical purity of the hydroperoxides is unknown and as a result the enantioselectivity of the reaction is impossible to quantitatively assess.

Dussault and Woller<sup>141</sup> reported a study of the dioxygenation of a variety of substrates using chiral phosphite ozonides derived from phosphites **119** and **120**. Conversion of the products into diastereomeric Mosher esters revealed a

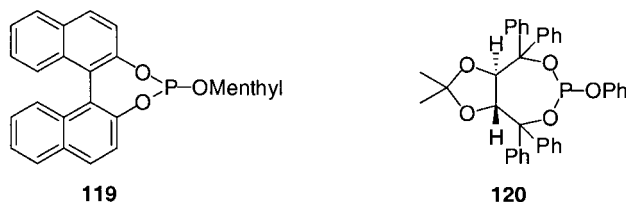


Scheme 53.



Scheme 54.

complete lack of enantioselectivity in the singlet oxygen ene reactions. These reactions were conducted under conditions which favored a bimolecular reaction between the ene substrate and the phosphite ozonide rather than via a singlet oxygen mechanism. Consequently, the lack of enantioselectivity suggests a reaction trajectory that bypasses steric interaction with the chiral auxiliaries on phosphorus. As a result of the small size of singlet oxygen, attempts to place the chiral auxiliary in the substrate to dramatically influence its enantioselectivity have also been unsuccessful.<sup>146</sup>



## 5. Conclusion and Practical Considerations

The strategies which have been discussed in this report were designed to provide control over the regio- and stereochemistry of singlet oxygen reactions thereby supplying the synthetic chemist with powerful tools for introduction of oxygen into organic substrates. A variety of different chemical and physical sources of singlet oxygen are available.<sup>6</sup> Sensitized photooxidations, however, are extremely convenient and can be conducted with polymer bound sensitizers which simplify reaction work-up.<sup>147</sup> The deleterious decomposition of the sensitizer can be avoided using 5, 10, 15, 20-tetrakis(heptafluoropropyl) porphyrin in a fluorous biphasic medium.<sup>148</sup> This protocol allows preparative scale photooxidations using inexpensive, recyclable, and environmentally benign reagents which can easily be separated from the products of the reaction.

## Acknowledgements

We thank the National Science Foundation and the donors of the Petroleum Research Fund, administered by the American Chemical Society, for their generous support of this research.

## References

- Fritzsche, M. *Compt. Rend.* **1867**, *64*, 1035–1037.
- Kautsky, H.; de Bruijn, H. *Naturwissenschaften* **1931**, *19*, 1043.
- Kautsky, H.; de Bruijn, H.; Neuwirth, R.; Baumeister, W. *Chem. Ber.* **1933**, *66*, 1588–1600.
- Kautsky, H. *Trans. Faraday Soc.* **1939**, *35*, 216–219.
- Schaap, A. P. In *Singlet Molecular Oxygen*, VanderWerf, C. A., Ed.; Dowden, Hutchinson & Ross: Stroudsburg, Pennsylvania, 1976; *5*, p 399.
- Wasserman, H. H.; Murray, R. W. In *Singlet Oxygen*, Wasserman, H. H., Ed.; Academic: New York, 1979; Vol. 40.
- Frimer, A. A. *Singlet O<sub>2</sub>*, CRC: Boca Raton, FL, 1985.
- Adam, W.; Prein, M. *Acc. Chem. Res.* **1996**, *29*, 275–283.
- Adam, W.; Brünker, H.-G.; Kumar, A. S.; Peters, E.-M.; Peters, K.; Schneider, U.; von Schnering, H. G. *J. Am. Chem. Soc.* **1996**, *118*, 1899–1905.
- Adam, W.; Saha-Möllner, C. R.; Schambony, S. B.; Schmid, K. S.; Wirth, T. *Photochem. Photobiol.* **1999**, *70*, 476–483.
- Adam, W.; Wirth, T. *Acc. Chem. Res.* **1999**, *32*, 703–710.
- Dussault, P. H.; Eary, C. T.; Lee, R. J.; Zope, U. R. *J. Chem. Soc. Perkin Trans. 1* **1999**, 2189–2204.
- Stratakis, M.; Orfanopoulos, M. *Tetrahedron* **2000**, *56*, 1595–1615.
- Schenck, G. O. *Naturwissenschaften* **1948**, *35*, 28–29.
- Frimer, A. A.; Stephenson, L. M. In *The Singlet Oxygen Ene Reaction*, Frimer, A. A., Ed.; CRC: Boca Raton, FL, 1985; Vol. II, pp 67–91.
- Hurst, J. R.; Wilson, S. L.; Schuster, G. B. *Tetrahedron* **1985**, *41*, 2191–2197.
- Gorman, A. A.; Hamblett, I.; Lambert, C.; Spencer, B.; Standen, M. C. *J. Am. Chem. Soc.* **1988**, *110*, 8053–8059.
- Song, Z.; Chrisope, D. R.; Beak, P. *J. Org. Chem.* **1987**, *52*, 3938–3940.
- Song, Z.; Beak, P. *J. Am. Chem. Soc.* **1990**, *112*, 8126–8134.
- Kopecky, K. R.; van de Sande, J. H. *Can. J. Chem.* **1972**, *50*, 4034–4049.
- Stephenson, L. M.; Grdina, M. J.; Orfanopoulos, M. *Acc. Chem. Res.* **1980**, *13*, 419–425.
- Grdina, S. B.; Orfanopoulos, M.; Stephenson, L. M. *J. Am. Chem. Soc.* **1979**, *101*, 3111–3112.
- Orfanopoulos, M.; Stephenson, L. M. *J. Am. Chem. Soc.* **1980**, *102*, 1417–1418.
- Rousseau, G.; LePerchec, P.; Conia, J. M. *Tetrahedron Lett.* **1977**, 2517–2520.
- Lerdal, D.; Foote, C. S. *Tetrahedron Lett.* **1978**, 3227–3230.
- Orfanopoulos, M.; Grdina, S. M. B.; Stephenson, L. M. *J. Am. Chem. Soc.* **1979**, *101*, 275–276.

27. Schulte-Elte, K. H.; Rautenstrauch, V. *J. Am. Chem. Soc.* **1980**, *102*, 1738–1740.
28. Inagaki, S.; Fujimoto, H.; Fukui, K. *Chem. Lett.* **1976**, 749–752.
29. Stephenson, L. M. *Tetrahedron Lett.* **1980**, *21*, 1005–1008.
30. Houk, K. N.; Williams Jr., J. C.; Mitchell, P. A.; Yamaguchi, K. *J. Am. Chem. Soc.* **1981**, *103*, 949–951.
31. Orfanopoulos, M.; Stratakis, M.; Elemes, Y.; Jensen, F. *J. Am. Chem. Soc.* **1991**, *113*, 3180–3181.
32. Adam, W.; Nestler, B. *Liebigs Ann. Chem.* **1990**, 1051–1053.
33. The more negative entropies of activation for the *trans* olefins could reflect the loss in rotational freedom of the vinyl substituents. The *cis* olefins, on the other hand, are already considerably organized, prior to the formations of their perepoxides, because of a gearing effect that restricts free rotation of the *cis* substituents.
34. Tanielian, C.; Mechin, R. *J. Phys. Chem.* **1988**, *92*, 265–267.
35. Jefford, C. W.; Boschung, A. F. *Helv. Chim. Acta* **1974**, *57*, 2242–2257.
36. Jefford, C. W.; Laffer, M. H.; Boschung, A. F. *J. Am. Chem. Soc.* **1972**, *94*, 8904–8905.
37. Clennan, E. L.; Matusuno, K. *J. Org. Chem.* **1987**, *52*, 3483–3485.
38. Paquette, L. A.; Carr, R. V. C.; Arnold, E.; Clardy, J. *J. Org. Chem.* **1980**, *45*, 4907–4913.
39. Lin, H.-S.; Paquette, L. A. *Synth. Commun.* **1986**, *16*, 1275–1283.
40. Ensley, H. E. In *Reactions of Singlet Oxygen with  $\alpha,\beta$ -Unsaturated Carbonyl Compounds*, Baumstark, A. L., Ed.; JAI: Greenwich, Connecticut, 1990; 2, pp 181–202.
41. Adam, W.; Griesbeck, A. *Angew. Chem. Int. Ed. Engl.* **1985**, *24*, 1070–1071.
42. Adam, W.; Catalani, L. H.; Griesbeck, A. *J. Org. Chem.* **1986**, *51*, 5494–5496.
43. Ensley, H. E.; Carr, R. V. C.; Martin, R. S.; Pierce, T. E. *J. Am. Chem. Soc.* **1980**, *102*, 2836–2838.
44. Kwon, B. M.; Kanner, R. C.; Foote, C. S. *Tetrahedron Lett.* **1989**, *30*, 903–906.
45. Ensley, H. E.; Balakrishnan, P.; Ugarkar, B. *Tetrahedron Lett.* **1983**, *24*, 5189–5192.
46. Adam, W.; Griesbeck, A. *Synthesis* **1986**, 1050–1052.
47. Orfanopoulos, M.; Foote, C. S. *Tetrahedron Lett.* **1985**, *26*, 5991–5994.
48. Clennan, E. L.; Chen, X.; Koola, J. J. *J. Am. Chem. Soc.* **1990**, *112*, 5193–5199.
49. Orfanopoulos, M.; Stratakis, M.; Elemes, Y. *J. Am. Chem. Soc.* **1990**, *112*, 6417–6419.
50. Orfanopoulos, M.; Stratakis, M.; Elemes, Y. *Tetrahedron Lett.* **1989**, *30*, 4875–4878.
51. Clennan, E. L.; Koola, J. J.; Oolman, K. A. *Tetrahedron Lett.* **1990**, *31*, 6759–6762.
52. Stratakis, M.; Orfanopoulos, M. *Synth. Commun.* **1993**, *23*, 425–430.
53. Adam, W.; Richter, M. J. *Tetrahedron Lett.* **1993**, *34*, 8423–8426.
54. Akasaka, T.; Misawa, Y.; Goto, M.; Ando, W. *Tetrahedron* **1989**, *45*, 6657–6666.
55. Fristad, W. E.; Bailey, T. R.; Paquette, L. A. *J. Org. Chem.* **1978**, *43*, 1620–1623.
56. Fristad, W. E.; Bailey, T. R.; Paquette, L. A.; Gleiter, R.; Böhm, M. C. *J. Am. Chem. Soc.* **1979**, *101*, 4420–4423.
57. Fristad, W. E.; Bailey, T. R.; Paquette, L. A. *J. Org. Chem.* **1980**, *45*, 3028–3037.
58. Adam, W.; Richter, M. J. *J. Org. Chem.* **1994**, *59*, 3335–3340.
59. Adam, W.; Klug, P. *J. Org. Chem.* **1993**, *58*, 3416–3420.
60. Adam, W.; Klug, P. *J. Org. Chem.* **1994**, *59*, 2695–2699.
61. Akasaka, T.; Takeuchi, K.; Misawa, Y.; Ando, W. *Heterocycles* **1989**, *28*, 445–451.
62. Akasaka, T.; Takeuchi, K.; Ando, W. *Tetrahedron Lett.* **1987**, *28*, 6633–6636.
63. Adam, W.; Brünker, H.-G.; Nestler, B. *Tetrahedron Lett.* **1991**, *32*, 1957–1960.
64. Eliel, E. L.; Wilen, S. H. *Stereochemistry of Organic Compounds*; Wiley: New York, NY, 1994.
65. Dussault, P. H.; Hayden, M. R. *Tetrahedron Lett.* **1992**, *33*, 443–446.
66. Dussault, P. H.; Woller, K. R.; Hillier, M. C. *Tetrahedron* **1994**, *50*, 8929–8940.
67. Adam, W.; Güthlein, M.; Peters, E.-M.; Peters, K.; Wirth, T. *J. Am. Chem. Soc.* **1998**, *120*, 4091–4093.
68. Hartman, G. D.; Traylor, T. G. *Tetrahedron Lett.* **1975**, 939–942.
69. Laporterie, A.; Dubac, J.; Mazerolles, P.; Loughmane, H. *J. Organomet. Chem.* **1981**, *216*, 321–329.
70. Laporterie, A.; Dubac, J.; Mazerolles, P. *J. Organomet. Chem.* **1980**, *202*, C89–C92.
71. Dubac, J.; Laporterie, A.; Loughmane, H. I.; Pillot, J. P.; Délérís, G.; Dunogués, J. *J. Organomet. Chem.* **1985**, *281*, 149–162.
72. Dubac, J.; Laporterie, A. *Chem. Rev.* **1987**, *87*, 319–334.
73. Laporterie, A.; Dubac, J.; Lesbre, M. *J. Organomet. Chem.* **1975**, *101*, 187–208.
74. Shimizu, N.; Shibata, F.; Imazu, S.; Tsuno, Y. *Chem. Lett.* **1987**, 1071–1074.
75. Okada, K.; Mukai, T. *J. Am. Chem. Soc.* **1978**, *100*, 6509–6510.
76. Paquette, L. A.; Hertel, L. W.; Gleiter, R.; Böhm, M. *J. Am. Chem. Soc.* **1978**, *100*, 6510–6512.
77. Hertel, L. W.; Paquette, L. A. *J. Am. Chem. Soc.* **1979**, *101*, 7620–7622.
78. Paquette, L. A.; Bellamy, F.; Wells, G. J.; Böhm, M. C.; Gleiter, R. *J. Am. Chem. Soc.* **1981**, *103*, 7122–7133.
79. Wu, Y.-D.; Li, Y.; Na, J.; Houk, K. N. *J. Org. Chem.* **1993**, *58*, 4625–4628.
80. Mehta, G.; Uma, R. *J. Org. Chem.* **2000**, *65*, 1685–1696.
81. Cieplak, A. S. *J. Am. Chem. Soc.* **1981**, *103*, 4540–4552.
82. Dang, H.-S.; Davies, A. G. *J. Chem. Soc. Perkin Trans. 2* **1991**, 2011–2020.
83. Dang, H.-S.; Davies, A. G. *Tetrahedron Lett.* **1991**, *32*, 1745–1748.
84. Dang, H.-S.; Davies, A. G. *J. Chem. Soc. Perkin Trans. 2* **1992**, 1095–1101.
85. Dang, H.-S.; Davies, A. G. *J. Organomet. Chem.* **1992**, *430*, 287–298.
86. Dussault, P. H.; Lee, R. J. *J. Am. Chem. Soc.* **1994**, *116*, 4485–4486.
87. Dussault, P. H.; Zope, U. R. *Tetrahedron Lett.* **1995**, *36*, 2187–2190.
88. Adam, W.; Kades, E.; Wang, X. *Tetrahedron Lett.* **1990**, *31*, 2259–2262.
89. Prein, M.; Adam, W. *Angew. Chem. Int. Ed. Engl.* **1996**, *35*, 477–494.
90. Adam, W.; Nestler, B. *J. Am. Chem. Soc.* **1992**, *114*, 6549–6550.
91. Adam, W.; Nestler, B. *J. Am. Chem. Soc.* **1993**, *115*, 5041–5049.

92. Adam, W.; Gevert, O.; Klug, P. *Tetrahedron Lett.* **1994**, *35*, 1681–1684.
93. Adam, W.; Brunker, H.-G. *J. Am. Chem. Soc.* **1993**, *115*, 3008–3009.
94. Brünker, H.-G.; Adam, W. *J. Am. Chem. Soc.* **1995**, *117*, 3976–3982.
95. For other examples of the ability of the proton donor/acceptor properties of the solvent to change the regiochemistry of the singlet oxygen ene reaction of allylic alcohols see the following reference and Ref. 96. Vassilikogiannakis, G.; Stratakis, M.; Orfanopoulos, M.; Foote, C. S. *J. Org. Chem.*, **1999**, *64* 4130–4139.
96. Stratakis, M.; Orfanopoulos, M.; Foote, C. S. *Tetrahedron Lett.* **1996**, *37*, 7159–7162.
97. Adam, W.; Nestler, B. *Tetrahedron Lett.* **1993**, *34*, 611–614.
98. Linker, T.; Frölich, L. *Angew. Chem. Int. Ed. Engl.* **1994**, *33*, 1971–1972.
99. The inability of a homoallylic alcohol to direct the attack of singlet oxygen is not universal. Exceptional diastereoselectivity has been reported in the photooxidation of a cyclohexadiene bearing a homoallylic alcohol substituent; Linker, T.; Frölich, L. *J. Am. Chem. Soc.*, **1995**, *117* 2694–2697. The cyclohexadienyl homoallylic alcohol is more rigid than **89**, however, it does point out the danger of assuming that only allylic substituents can influence the direction of singlet oxygen attack.
100. Adam, W.; Prein, M. *J. Am. Chem. Soc.* **1993**, *115*, 3766–3767.
101. Adam, W.; Prein, M. *Tetrahedron Lett.* **1994**, *35*, 4331–4334.
102. Adam, W.; Peters, E. M.; Peters, K.; Prein, M.; von Schnering, H. C. *J. Am. Chem. Soc.* **1995**, *117*, 6686–6690.
103. Prein, M.; Maurer, M.; Peters, E. M.; Peters, K.; von Schnering, H. G.; Adam, W. *Chem. Eur. J.* **1995**, *1*, 89–94.
104. Adam, W.; Saha-Möllner, C. R.; Schambony, S. B. *J. Am. Chem. Soc.* **1999**, *121*, 1834–1838.
105. Gollnick, K.; Griesbeck, A. *Tetrahedron Lett.* **1984**, *25*, 725–728.
106. Ando, W.; Watanabe, K.; Suzuki, J.; Migita, T. *J. Am. Chem. Soc.* **1974**, *96*, 6766–6768.
107. Manring, L. E.; Foote, C. S. *J. Am. Chem. Soc.* **1983**, *105*, 4710–4717.
108. Orfanopoulos, M.; Stratakis, M. *Tetrahedron Lett.* **1991**, *32*, 7321–7324.
109. Stratakis, M.; Orfanopoulos, M.; Foote, C. S. *J. Org. Chem.* **1998**, *63*, 1315–1318.
110. Sen, S. E.; Smith, S. M.; Sullivan, K. A. *Tetrahedron* **1999**, *55*, 12657–12698.
111. Ramamurthy, V.; Sanderson, D. R.; Eaton, D. F. *J. Am. Chem. Soc.* **1993**, *115*, 10438–10439.
112. Li, X.; Ramamurthy, V. *J. Am. Chem. Soc.* **1996**, *118*, 10666–10667.
113. Foote, C. S. *Photochem. Photobiol.* **1991**, *54*, 659.
114. Li, X.; Ramamurthy, V. *Tetrahedron Lett.* **1996**, *37*, 5235–5238.
115. Shailaja, S.; Sivaguru, J.; Robbins, R. J.; Ramamurthy, V.; Sunoj, R. B.; Chandrasekhar, J. *Tetrahedron* **2000**, submitted.
116. Robbins, R. J.; Ramamurthy, V. *J. Chem. Soc. Chem. Commun.* **1997**, 1071–1072.
117. Ramamurthy, V.; Lakshminarasimhan, P.; Grey, C. P.; Johnston, L. J. *J. Chem. Soc. Chem. Commun.* **1998**, 2411–2424.
118. Clennan, E. L.; Sram, J. P. *Tetrahedron Lett.* **1999**, *40*, 5275–5278.
119. No product from abstraction of hydrogen from the allylic methylene group was observed either in solution or in the zeolite.
120. Clennan, E. L.; Sram, J. reported at the National American Chemical Society meeting; New Orleans, LA, August 22–26, 1999.
121. Stratakis, M.; Froudakis, G. *Org. Lett.* **2000**, *2*, 1369–1372.
122. Clennan, E. L.; Sram, J. P. *Tetrahedron* **2000**, *56*, 6945–6950.
123. Shailaja, J.; Ponchot, K. J.; Ramamurthy, V. *Org. Lett.* **2000**, *2*, 937–940.
124. Joy, A.; Scheffer, J. R.; Ramamurthy, V. *Org. Lett.* **2000**, *2*, 119–121.
125. Joy, A.; Robbins, R. J.; Pitchumani, K.; Ramamurthy, V. *Tetrahedron Lett.* **1997**, *38*, 8825–8828.
126. Tung, C.-H.; Wang, H.; Ying, Y.-M. *J. Am. Chem. Soc.* **1998**, *120*, 5179–5186.
127. The opposite process of generating singlet oxygen in the zeolite and its diffusion into solution where it reacts with a substrate with ‘normal selectivity’ has also been reported. Pettit, T. L.; Fox, M. A. *J. Phys. Chem.*, **1986**, *90* 1353–1354.
128. Frimer, A. A.; Bartlett, P. D.; Boschung, A. F.; Jewett, J. G. *J. Am. Chem. Soc.* **1977**, *99*, 7977–7986.
129. Chan, Y.-Y.; Li, X.; Zhu, C.; Liu, X.; Zhang, Y.; Leung, H.-K. *J. Org. Chem.* **1990**, *55*, 5497–5504.
130. Lissi, E.; Rubio, M. A. *Pure Appl. Chem.* **1990**, *62*, 1503–1510.
131. Ehrenberg, B.; Anderson, J. L.; Foote, C. S. *Photochem. Photobiol.* **1998**, *68*, 135–140.
132. Lissi, E. A.; Encinas, M. V.; Lemp, E.; Rubio, M. A. *Chem. Rev.* **1993**, *93*, 699–723.
133. Hovey, M. C. *J. Am. Chem. Soc.* **1982**, *104*, 4196–4202.
134. Horsey, B. E.; Whitten, D. G. *J. Am. Chem. Soc.* **1978**, *100*, 1293–1295.
135. Ohtani, B.; Nishida, M.; Nishimoto, S.; Kagiya, T. *Photochem. Photobiol.* **1986**, *44*, 725–732.
136. Lee, P. C.; Rodgers, M. A. J. *J. Phys. Chem.* **1984**, *88*, 4385–4389.
137. Niu, E. P.; Mau, A. W. H.; Ghiggino, K. P. *Aust. J. Chem.* **1991**, *44*, 695–704.
138. Tung, C.-H.; Guan, J.-Q. *J. Am. Chem. Soc.* **1998**, *120*, 11874–11879.
139. Foote, C. S. *Tetrahedron* **1985**, *41*, 221–2227.
140. Hurst, J. R.; McDonald, J. D.; Schuster, G. B. *J. Am. Chem. Soc.* **1982**, *104*, 2065–2067.
141. Dussault, P. H.; Woller, K. R. *J. Org. Chem.* **1997**, *62*, 1556–1559.
142. Kuroda, Y.; Sera, T.; Ogoshi, H. *J. Am. Chem. Soc.* **1991**, *113*, 2793–2794.
143. Kuroda, Y.; Hiroshige, T.; Sera, T.; Shirowa, Y.; Tanaka, H.; Ogoshi, H. *J. Am. Chem. Soc.* **1989**, *111*, 1912–1913.
144. Weber, L.; Imiolczyk, I.; Haufe, G.; Rehorek, D.; Henning, H. *J. Chem. Soc. Chem. Commun.* **1992**, 301–303.
145. Gerdil, R.; Barchetto, G. *J. Am. Chem. Soc.* **1984**, *106*, 8004–8005.
146. Adam, W.; Wirth, T.; Pastor, A.; Peters, K. *Eur. J. Org. Chem.* **1998**, 501–506.
147. Schaap, A. P.; Thayer, A. L.; Blosssey, E. C.; Neckers, D. C. *J. Am. Chem. Soc.* **1975**, *97*, 3741–3745.
148. DiMagno, S. G.; Dussault, P. H.; Schultz, J. A. *J. Am. Chem. Soc.* **1996**, *118*, 5312–5313.

**Biographical Sketch**



**Edward L. Clelman** was born in 1951 in St. Paul Minnesota. He received his BS degree in chemistry and mathematics from the University of Wisconsin at River Falls and his PhD from the University of Wisconsin at Madison. Prior to joining the faculty at the University of Wyoming he spent two years at Texas Christian University working as a postdoctoral fellow in the laboratory of Professor P. D. Bartlett. In addition, in recent years he spent a year at the National Science Foundation as a program officer and three years as Head of the Department of Chemistry at the University of Wyoming where he is currently a Professor of Chemistry. His research interests are in the area of oxidation chemistry in homogeneous and heterogeneous media. Current projects include the study of singlet oxygen reactions in zeolites and the development of new mechanistic tools to study organic reactions in heterogeneous media.